U. S. ARMY
TRANSPORTATION RESEARCH COMMAND
FORT EUSTIS, VIRGINIA

TCREC TECHNICAL REPORT 62-93

EVALUATION OF A HELICOPTER-FUSELAGE-MOUNTED DYNAMIC-NEUTRALIZER STATIC ELECTRICITY DISCHARGING SYSTEM

Task 1D121401A14130
(Formerly Task 9R38-01-017-30)
Contract DA 44-177-TC-843

December 1962

prepared by:

KELLETT AIRCRAFT CORPORATION
Willow Grove, Pennsylvania

DISCLAIMER NOTICE

When Government drawings, specifications, or other data are used for any purpose other than in connection with a definitely related Government procurement operation, the United States Government thereby incurs no responsibility nor any obligation whatsoever; and the fact that the Government may have formulated, furnished, or in any way supplied the said drawings, specifications, or other data is not to be regarded by implication or otherwise as in any manner licensing the holder or any other person or corporation, or conveying any rights or permission, to manufacture, use, or sell any patented invention that may in any way be related thereto.

* * * *

ASTIA AVAILABILI' NOTICE

Qualified requesters may obtai : :opies of this report from

Armed Services Technical Information Agency
Arlington Hall Station
Arlington 12, Virginia

* * * *

This report has been released to the Office of Te-hnical Service, U. S. Department of Commerce, Washington 25, D. C., for sale to general public.

* * * *

The findings and recommendations contained in this report are those of the Contractor and do not necessarily reflect the views of the U. S. Army Mobility Command, the U. S. Army Material Command, or the Department of the Army.

* * * *

The information contained herein will not be used for advertising purposes.

BLANK PAGE

HEADQUARTERS
U. S. ARMY TRANSPORTATION RESEARCH COMMAND
Fort Eustis, Virginia

This report has been reviewed by the Transportation Research Command and is technically sound. It is published for the exchange of information and stimulation of ideas.

The conclusions and recommendations made by the contractor are considered to be valid by this Command.

FOR THE COMMANDER:

KENNETH B. ABEL
Captain, TC
Adjutant

Approved by:

S. Blair Poteate, Jr.
S. BLAIR POTEATE, JR.
Project Engineer

Task 1D121401A14130
(Formerly Task 9R38-01-017-30)
Contract DA 44-177-TC-843
TCREC Technical Report 62-93
December 1962

EVALUATION OF A HELICOPTER-FUSELAGE-MOUNTED DYNAMIC-NEUTRALIZER STATIC ELECTRICITY DISCHARGING SYSTEM

Prepared by

KELLETT AIRCRAFT CORPORATION
Willow Grove, Pennsylvania

for
U. S. ARMY TRANSPORTATION RESEARCH COMMAND
FORT EUSTIS, VIRGINIA

PREFACE

The Kellett Aircraft Corporation, with the sponsorship of the U. S. Army Transportation Research Command, Fort Eustis, Virginia, has conducted a research program under Contract No. DA 44-177-TC-843 to evaluate a helicopter-fuselage-mounted static electricity discharging system. The principal investigator has been Mr. Juan de la Cierva and the cognizant TRECOM project officer was Mr. S. Blair Poteate, Jr.

This research conducted from January to July 1962, was the continuation of successful research of helicopter static electricity discharging systems conducted under Contract No. DA 44-177-TC-728 from June to December 1961 under sponsorship of the U. S. Army Transportation Research Command.

Flight tests were conducted by the Army Aviation Office at Edwards Air Force Base, California, during April and May 1962.

The cooperation of the Army aviation personnel pursuant to the completion of this program and the assistance of the Thompson-Ramo-Wooldridge Corporation in providing a DC generator are hereby acknowledged.

CONTENTS

LIST OF TABLES

LIST OF ILLUSTRATIONS

Figure	Title	Page
17	Dynamic Neutralizer Performance, Tail and Exhaust Corona Points	39
18	Dynamic Neutralizer Performance, Generator Voltage vs. Helicopter Voltage Plot	40
19	Dynamic Neutralizer Voltage Output vs. Voltage Input	41

SUMMARY

A static electricity discharging system, known as the dynamic neutralizer, has been designed, built and flight-tested, and the results are presented herein. The dynamic neutralizer had been previously tested in a rotor-blade-mounted version as reported in Reference 1. The program discussed in the present report was concerned with the evaluation of this discharger when installed in the fuselage of an Army H-37 helicopter.

The test data confirm that the principle of operation of the dynamic neutralizer is not affected by locating the entire device in the fuselage.

The dynamic neutralizer utilized in this program was tested with generator voltages up to 60 kilovolts. With this voltage, the H-37 helicopter, operating under the natural charging conditions prevailing at the test site, was discharged to a minimum energy level of 3.4 millijoules from the estimated 1000 millijoules present in the helicopter before the discharger was put into operation. It appears, however, that better performance will be required for operational purposes. It is recommended, therefore, that further research be conducted toward achieving the required performance.

Several problems arose in the electrical operation used for these tests. However, data in sufficient quantity have been obtained for the purpose of evaluating the system capabilities and the performance of corona points.

CONCLUSIONS

The evaluation of the data obtained in this program resulted in the following conclusions:

1. The dynamic neutralizer static electricity discharging system, in the configuration tested in the present program, and under the natural charging current conditions prevailing at the test site, reduces the electrostatic energy stored in the helicopter from a level of 1000 millijoules down to a minimum level of 3.4 millijoules. Improved performance may be required for operational use according to objectives set forth in References 1 and 3.

2. The performance of the discharging device used for this program could be improved by increasing the corona point length in the tail-mounted corona point configuration. An extrapolation of the data indicates that the dynamic neutralizer, operating at 80 kilovolts and using 5-foot-long tail-mounted points, would decrease the electrostatic level on the helicopter to 0.35 millijoule with a 2-4 microampere charging condition.

3. The dynamic neutralizer provides a method of sensing the presence of electrostatic charge on the aircraft, by measuring the differential current flowing through the two high-voltage corona points of the device.

4. A high-voltage corona point operating at voltages of 60 kilovolts, and installed 24 inches aft of the exhaust nozzle of an H-37 engine, can generate a discharging current up to 29 microamperes.

5. Information has come to the attention of this Contractor during the performance of this contract that natural charging currents up to 50 microamperes have been measured in certain geographic areas of operational interest for large helicopters. In addition, natural charging currents up to 22 microamperes have been measured with the H-37 helicopter operating below ten feet at Edwards Air Force Base, whereas at higher altitudes (25 feet) the natural charging current reaches only 2 to 4 microamperes. The dust and sand recirculation through the rotor disc at lower altitudes seems to account for the resultant increased natural charging current.

These facts, in conjunction with the results of the measurements performed on the fuselage-mounted dynamic neutralizer, leads to the conclusion that the discharging configuration tested, in a fuselage-mounted version, will not provide complete protection from electrostatic charge under all conditions that will be encountered with helicopter operations.

6. Further research is required to obtain a discharging system commensurate with anticipated operational needs.

I. INTRODUCTION

Experience has shown that the accumulation of static electricity seriously affects the operational capabilities of helicopters. The topic of electrostatic discharging has become, therefore, of increased interest in recent years. This interest was furthered by the U. S. Army Transportation Research Command which has sponsored a number of research programs designed to increase the knowledge of electrostatic charging and discharging phenomena. The results of one of these programs is reported in Reference 1. The research of Reference 1 concerned the design and flight test of a rotor-blade-mounted discharger which successfully reduced the electrostatic energy accumulating in an H-37 helicopter to an acceptable level. These tests were performed at Edwards Air Force Base, California, under natural charging current in the range of 2 microamperes. The discharger, called the dynamic neutralizer, utilized active corona points mounted on the rotor blades together with two 20-kilovolt DC generators.

Because of a number of practical reasons, it was considered desirable to locate the entire discharging system in the helicopter fuselage. The U. S. Army TRECOM, therefore, sponsored a follow-on program with the objective of evaluating the feasibility and performance of a fuselage-mounted dynamic neutralizer. The present report presents the results of this latter program.

II. DISCUSSION OF THE PROBLEM

A. INTRODUCTION

The program described herein consists of the design and test of a static electricity discharger known as the dynamic neutralizer. Figure 1 is a photograph of the test aircraft parked on the ramp at Edwards Air Force Base and Figure 2 shows the aircraft during one of the test flights.

A similar device installed in the rotor blades of the same type of aircraft was tested previously as reported in Reference 1. The principle of operation of the dynamic neutralizer is described in detail in Reference 1 and, hence, need not be repeated here.

The data presented in Reference 1 indicated that the performance of the dynamic neutralizer is highly dependent on the air flow around the corona points. It was realized that the placing of corona points at any location on the fuselage would result in substantially reduced velocities compared to those obtainable with rotor-blade-mounted probes. It was anticipated that the resulting performance decrease of the discharger could be compensated for by a suitable increase of generator voltages. Since no adequate theory existed on the effect of air velocity, generator voltage and other pertinent parameters on the performance of the discharger, certain assumptions had to be made for the determination of the design magnitudes. These assumptions are discussed subsequently in more detail.

B. PROGRAM OBJECTIVES

The objectives of this program were twofold:

1. To design, build and test a fuselage-mounted system to discharge an H-37 helicopter, generating a natural charging current of 20 microamperes, to an energy level below 1 millijoule. This energy level is considered to be satisfactory in accordance with References 1 and 3.

2. To obtain adequate test data to evaluate the importance of several design parameters on the performance of the dynamic neutralizer and its components.

The parameters investigated were:

FIGURE 1: THE H-37 TEST HELICOPTER ON THE RAMP

FIGURE 2: THE H-37 TEST HELICOPTER IN FLIGHT

1. Corona point location
2. Corona point length
3. Generator voltage.

To achieve the test objectives, twelve different corona point probe configurations were investigated. These configurations consisted of four locations and three probe lengths for each location.

Figure 3 illustrates the location of the probes in the test aircraft. The following reasons dictated the selection of the four chosen locations:

1. Nose Location

The possibility of studying the interaction between corona points was the principal argument favoring this configuration. The nose location satisfied the additional requirement of being symmetrical with respect to the aircraft geometry.

2. Engine Cowling Location

This configuration should provide a minimum of interference between both corona points, due to the large distance between them, while at the same time satisfying the requirement of being beyond the reach of ground personnel.

3. Tail Location

This location was chosen because it lies in a region of high rotor downwash air speed. This air speed was on the order of 100-200 feet per second as estimated in Reference 2.

4. Engine Exhaust Location

The objective in choosing this location was to utilize the exhaust gas speed to increase the corona point performance. No exact data on the actual gas speed on the corona point was obtained, but this speed is estimated to be in the range between 100 and 300 feet per second depending on the distance of the probe aft of the exhaust nozzle.

It should be noted that all of these locations satisfied the requirement of being beyond the reach of ground personnel.

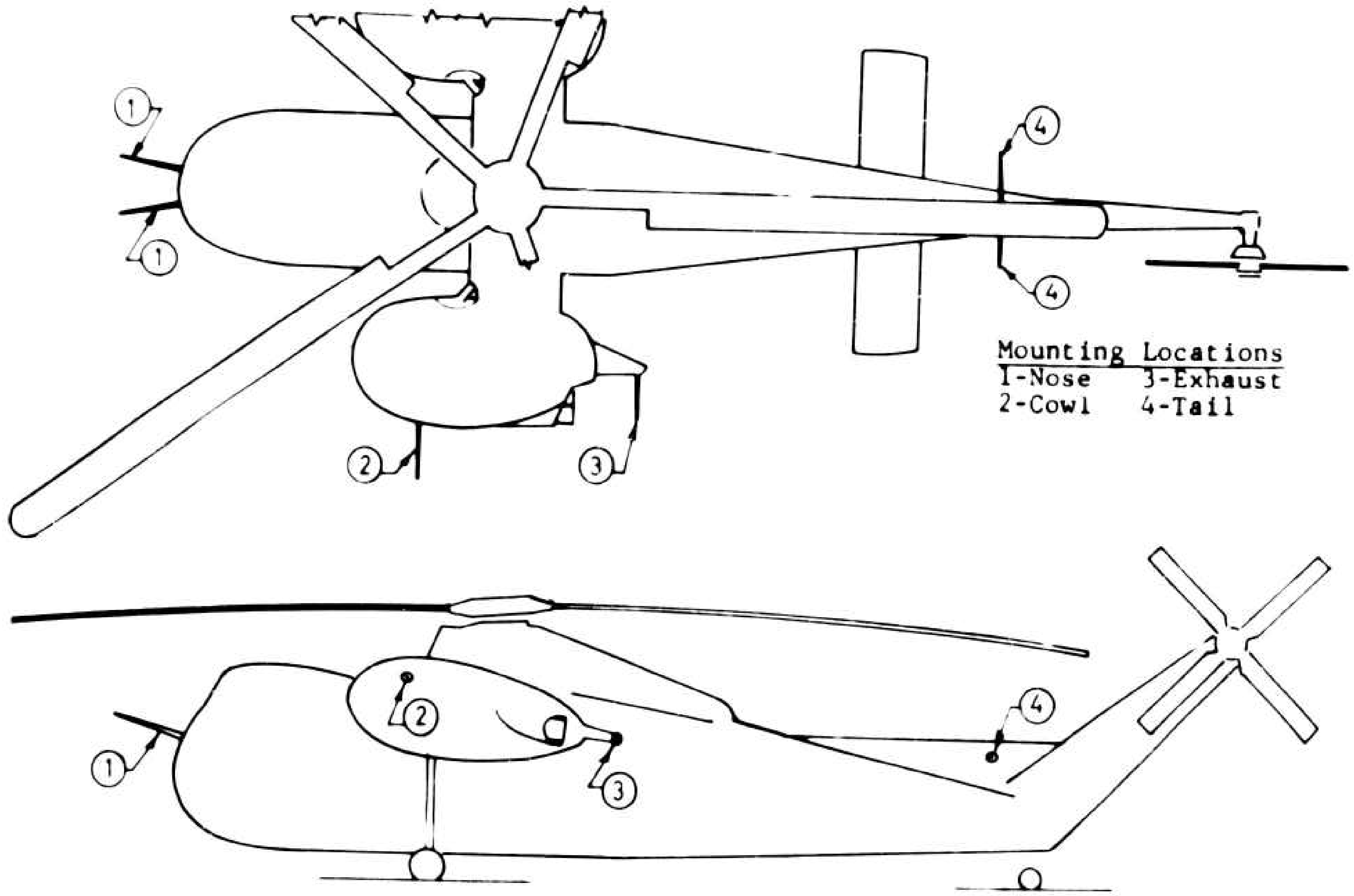

FIGURE 3: H-37 HELICOPTER THREE-VIEW DRAWING, SHOWING THE LOCATION OF THE CORONA POINTS

Figures 4 and 5 are photographs of the tail and engine exhaust corona point installations, respectively. Figure 4 shows the 3-foot long corona point, while Figure 5 shows the point installed 4 feet aft of the exhaust nozzle.

The range of corona point length chosen for this program was between 2 and 4 feet. Sparking between the point and the helicopter fuselage dictated the lower limit of this range, whereas the upper limit was chosen because of practical corona point size considerations.

In order to determine the effect of the corona point operating voltage on the performance of the discharging system, the high-voltage generator was designed with provisions to adjust its output voltages between 20 and 80 kilovolts. The design of the units, which will be described in the next section of this report, was such that any voltage change affected simultaneously both high-voltage outputs. In this manner, the balance of the dynamic neutralizer was automatically maintained through the operative range of the instrument.

The importance of the previously mentioned parameters on the system performance was evaluated in terms of the energy level remaining in the aircraft for a given discharger configuration. The energy is measured according to:

$$W = \tfrac{1}{2}CV^2 \qquad (1)$$

where

W is the helicopter-stored electrostatic energy, in joules

C is the helicopter capacitance, in farads

V is the helicopter-to-ground voltage, in volts.

The energy stored in the helicopter is a quantity that is difficult to measure. But as noted from Equation (1), the energy level for a given capacitance can also be determined by the voltage remaining in the aircraft. The data of Reference 1 show that an H-37 helicopter hovering at 25 feet has a capacitance of approximately 670 micro-micro farads. It follows from Equation (1) that the voltage corresponding to 1 millijoule of stored energy is equal to 1645 volts. This voltage, therefore, was considered to be the maximum satisfactory level of helicopter-to-ground potential.

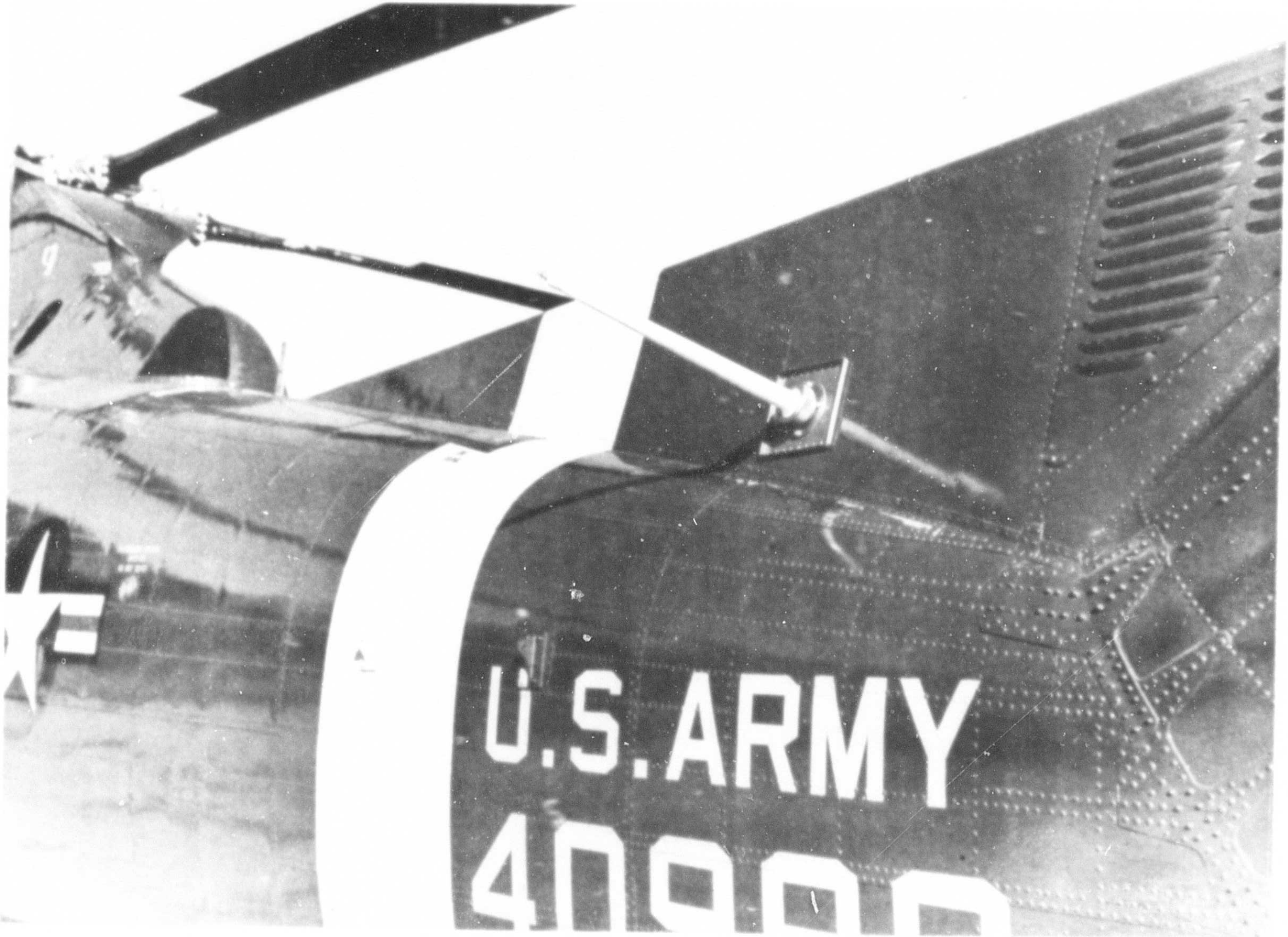

FIGURE 4: CORONA POINT MOUNTED ON THE TAIL OF THE H-37 TEST HELICOPTER

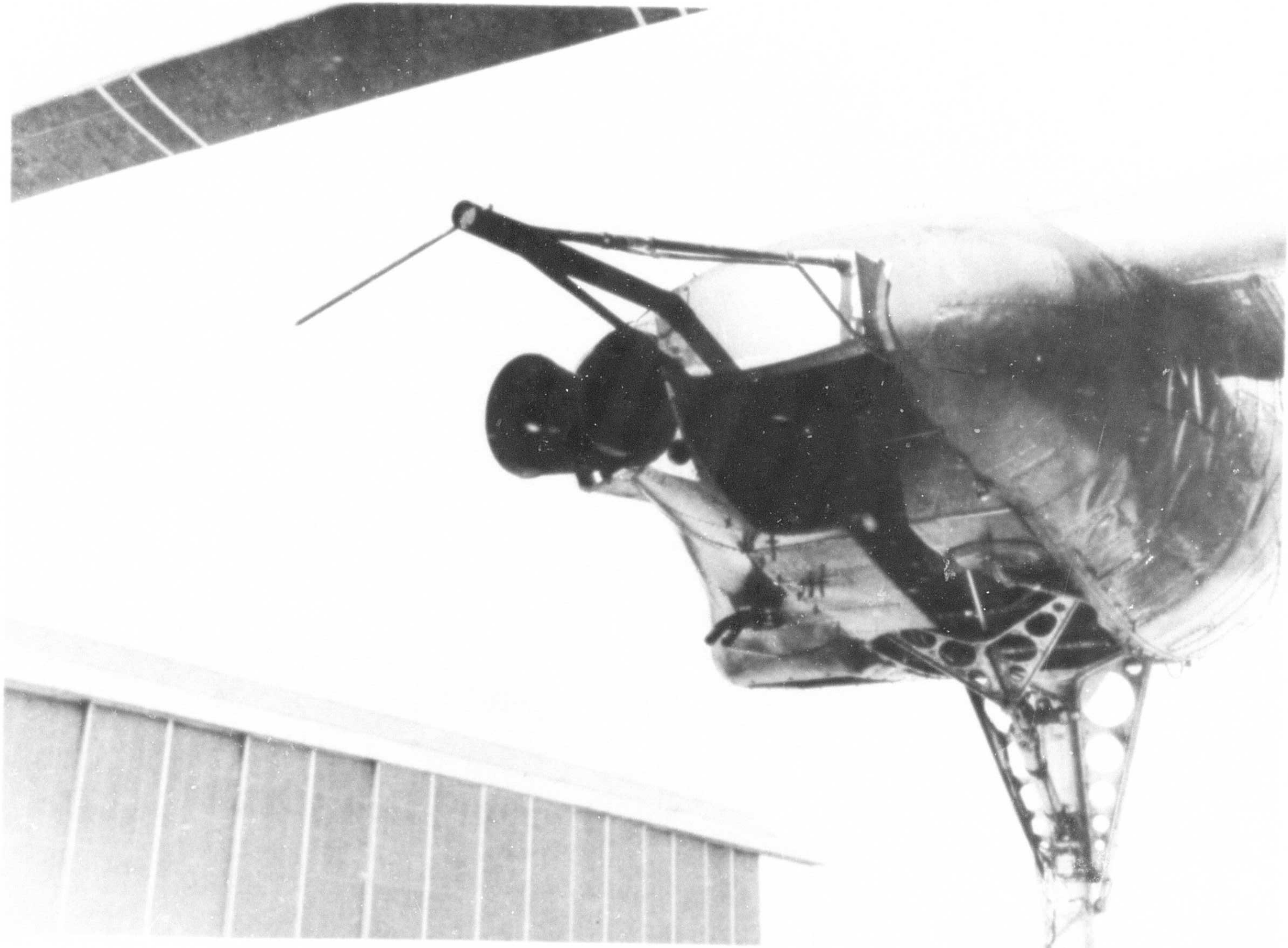

FIGURE 5: CORONA POINT MOUNTED IN THE ENGINE EXHAUST OF THE H-37 TEST

During the flight test program, considerable attention was given to the measurement of the performance (current vs. voltage) of corona points. One reason for this attention was the fact that the performance of the dynamic neutralizer was expected to be a function of the corona point current as well as the slope of the curve of corona point voltage vs. current for every configuration and operating voltage. In addition, Reference 3, published after the starting date of the present contract, reports natural charging currents up to 50 microamperes for H-37 aircraft operated at Fort Greeley, Alaska, in snow-laden atmosphere. This implies that any static electricity discharger designed to reduce the helicopter voltage to a satisfactory value for the above level of natural charging, must have corona points with a total discharging capability of 50 microamperes or higher. Hence, the investigation of corona point performance was by itself considered of great importance for future static discharger research.

C. TEST EQUIPMENT

1. Dynamic Neutralizer

The results of the test data presented in Reference 1 showed that the performance of the corona points is dependent on two major factors:

a. Local air speed
b. Generator voltage.

In addition, the performance of the dynamic neutralizer system is affected by the electrostatic field created by the charged aircraft in the vicinity of the corona point as well as by the natural charging current.

As pointed out previously, the locating of the corona points on the fuselage results in a reduction of air speed. In addition, the level of natural charging current that was to be eliminated was specified as 20 microamperes. To compensate for the resulting corona point performance, the generator voltage was to be increased and the points were to be located in a lower aircraft electrostatic field. Since no theory was available for determining the required design magnitude of the generator voltage, the assumption was made that all parameters affect the performance of the dynamic neutralizer in a linear manner. The generator voltage magnitude was approached as shown below:

Parameter	Ref. 1 Value	Design Value	Voltage Design Factor
Air Speed (ft./sec.)	400	150	2.67
Corona Point (ft.)	1	4	0.25
Natural Charging Current (microamperes)	2	20	10.00
Aircraft Field			0.50 (Estimated)

The required voltage was obtained by multiplying the voltage used in Reference 1 (20 kilovolts) by the resulting voltage design factor. The voltage design factor, V.D.F., is given by

$$V.D.F. = (2.67)(0.25)(10.0)(0.5) = 3.34$$

Consequently the required voltage for the generators used in this program was 66.8 kilovolts. Actually, a design value of 80 kilovolts was chosen.

Construction of the dynamic neutralizer is in accordance with Figure 6, an electrical schematic diagram of the dynamic neutralizer. In addition, spare parts of the discharging unit were procured and assembled as a spare unit. The primary circuit is a standard saturated transformer-type transistorized oscillator, designed to operate at 24-28 volts, DC input. The secondary winding of the transformer was designed to supply a maximum peak voltage of 40 kilovolts. The transformer output was fed into two-voltage-doubling circuits connected with opposite polarity, giving an 80-kilovolt maximum DC output at 150 microamperes.

The design of the high-voltage units has the following characteristics:

a. The positive and negative outputs are identical by design, due to the fact that both are powered by the same AC source. The load resistance is chosen in such a manner that the reverse leakage current in the rectifying elements is at least one order of magnitude lower than the load current, thus insuring identical voltages in both positive and negative outputs.

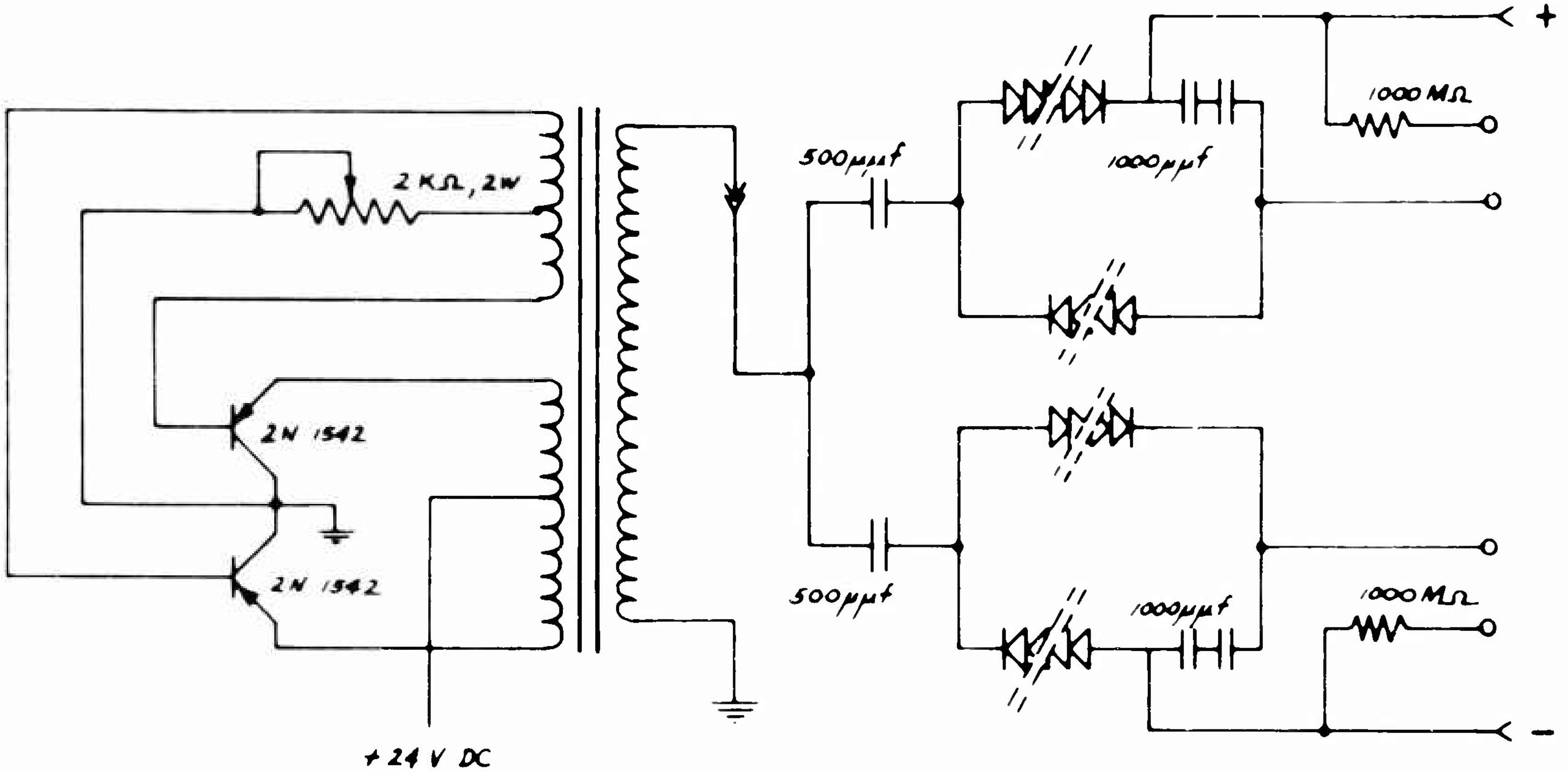

Symbols:

High-voltage male connector.
High-voltage female connector.
Series of high-voltage diodes.

FIGURE 6: DYNAMIC NEUTRALIZER SCHEMATIC DIAGRAM

b. The output voltage can be adjusted between 20 and 80 kilovolts by use of a variable resistor located in the common path of the transistor feedback current. The power requirements of the control potentiometer are sufficiently low to permit the use of a simple and inexpensive component to perform the control function.

c. The design of the secondary circuit is such that one of the sides of the high-voltage winding of the transformer is very close to ground potential. In this manner, the isolation requirements imposed on the transformer high-voltage winding are very moderate in the low-voltage side of the coil, thus simplifying the manufacture of the high-voltage transformer.

Both the high-voltage transformer and the complete voltage doubling circuits were encapsulated in transparent silicon rubber. The encapsulating agent used was the General Electric LTV-602 Clear Silicon Potting Compound. The dielectric strength of this material is 75 kilovolts per one tenth of an inch (ASTM Method D-176, 60 cycle, 1000 v/sec. rise, 0.5" spherical electrode), and this figure was used for the design of the unit together with a suitable safety factor.

The operation of the high-voltage generators during the test program was far from satisfactory. A continued succession of failures hindered the process of flight testing of the system. All of the failures were located on the high-voltage doubler circuits and were generally due to insulation failures, although the subsequent sparks in the circuit created transients leading to component (diode and capacitor) failures.

The reason for the insulation breakdown is not fully understood at this time. One explanation of this phenomenon appears to be the following:

Due to the low mechanical rigidity of the potting compound, together with the relatively high vibration level at which the unit was operated, a thin layer of air could form around the encapsulated components. This would happen if the components are not properly bonded to the potting compound. The resultant gas jacket would provide a path to initiate a spark, and the ozone and subsequent high-voltage transients would complete the circuit failure. The fact that the units were laboratory tested at full rating, and afterwards the maximum attainable voltage had to be reduced as the testing progressed, appears to support the preceding hypothesis.

However, it is believed that only a complete laboratory investigation and further testing will provide a conclusive answer for the reasons of the experienced failures.

2. Test Instrumentation

Table 1 lists the test equipment which has been used for this program. Figure 7 is a photograph of the instrumentation setup as installed in the aircraft.

As mentioned previously the basic measurements to be obtained in the test program consisted of the voltage of the H-37 helicopter equipped with an operating dynamic neutralizer. In addition, part of the test program was directed toward measuring the current discharging capability of twelve geometrically different corona point configurations operating at voltages up to 80,000 volts. Equipment problems limited the actual testing to a maximum voltage of 60,000 volts.

The operation of the dynamic neutralizer was monitored by measuring and recording the aircraft-to-ground voltage with the unit in operation. The range of interest in the voltage readings was 0 to 10,000 volts because any voltage above 10 kilovolts implies a clearly hazardous situation, as discussed in References 1 and 3. The input impedance of the voltmeter was 10^{12} ohms. This figure is at least one order of magnitude higher than the equivalent impedance of the helicopter static electricity generation process. This insures voltage readings of accuracy of more than 90%, which is believed to be sufficient for the goals of this program. The voltmeter used (Keithley Model 200) was equipped with recorder terminals. This output was used to obtain records of the helicopter voltage.

Figure 8 describes the test circuit utilized to measure corona point performance using the unit built under the present contract. The highest voltage reached with this unit was 46 kilovolts. Figure 9 describes the circuit used to measure the corona point performance, using a NJE, 120-kilovolt DC generator or Spellman 60-kilovolt generator.

Figure 10 is a schematic diagram of the circuit utilized to measure the performance of the dynamic neutralizer. Two twin channel recorders were used in this testing with the following channel assignments:

Channel A Positive high-voltage generator current.

Channel B Negative high-voltage generator current.

TABLE 1

LIST OF THE FLIGHT TEST INSTRUMENTATION

Quantity	Description	Make	Model
2	Direct writing, 2 channel recording oscillograph	Brush Instruments	BL-221
1	Dual channel DC amplifier	Brush Instruments	BL-928
2	Universal amplifiers	Brush Instruments	BL-520
1	Electrometer voltmeter	Keithley Instruments	200
1	Voltage divider	Keithley Instruments	2007
1	High-voltage DC power supply	Spellman High Voltage Co.	LAB-60-PN
1	High-voltage power supply	N J E	H-80
2	Microammeters, D-100 A	Weston Instruments	961
1	Microammeter, 20-0-20 A	Weston Instruments	201/301

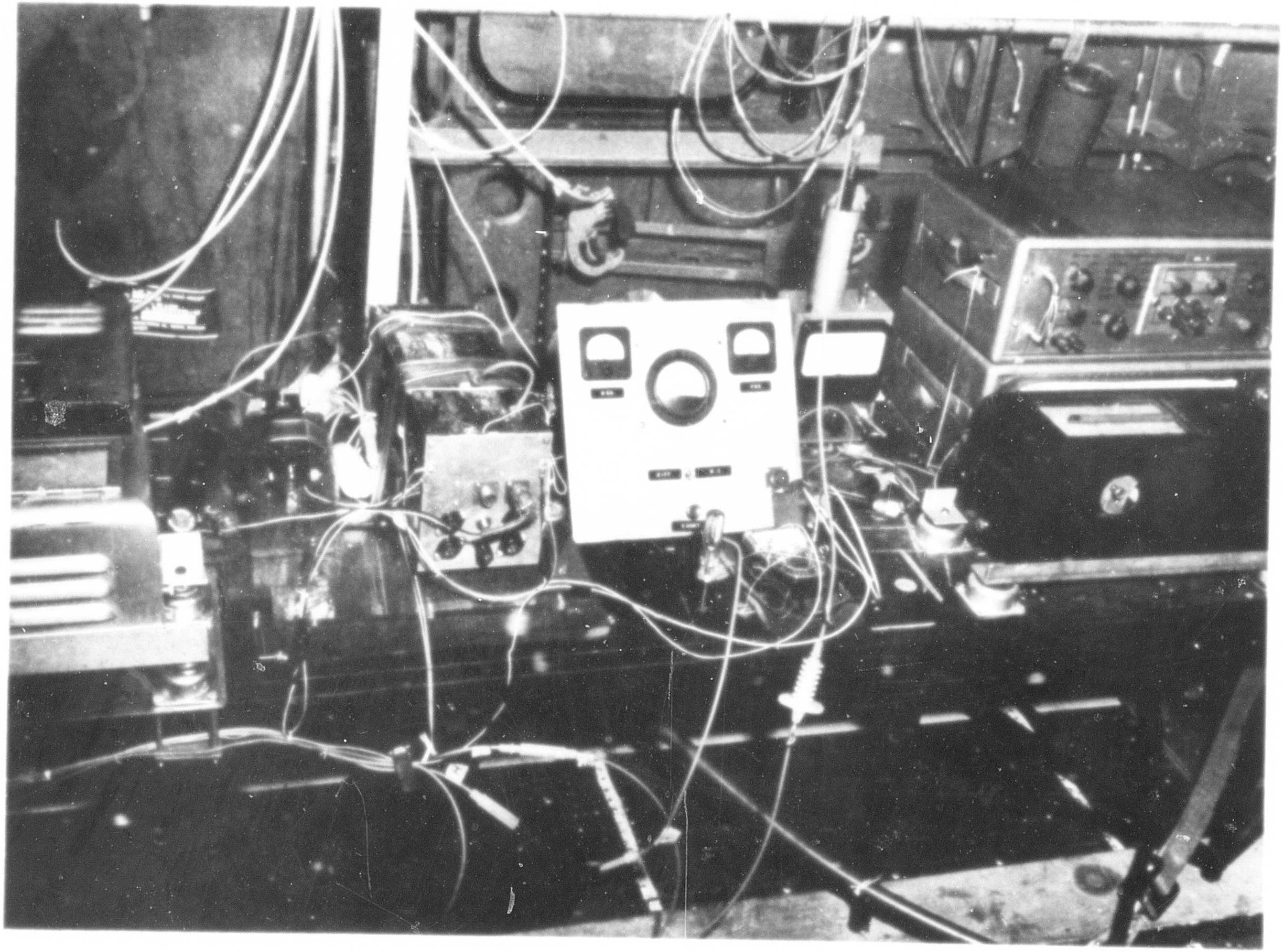

FIGURE 7: THE TEST INSTRUMENTATION ABOARD THE H-37 TEST HELICOPTER

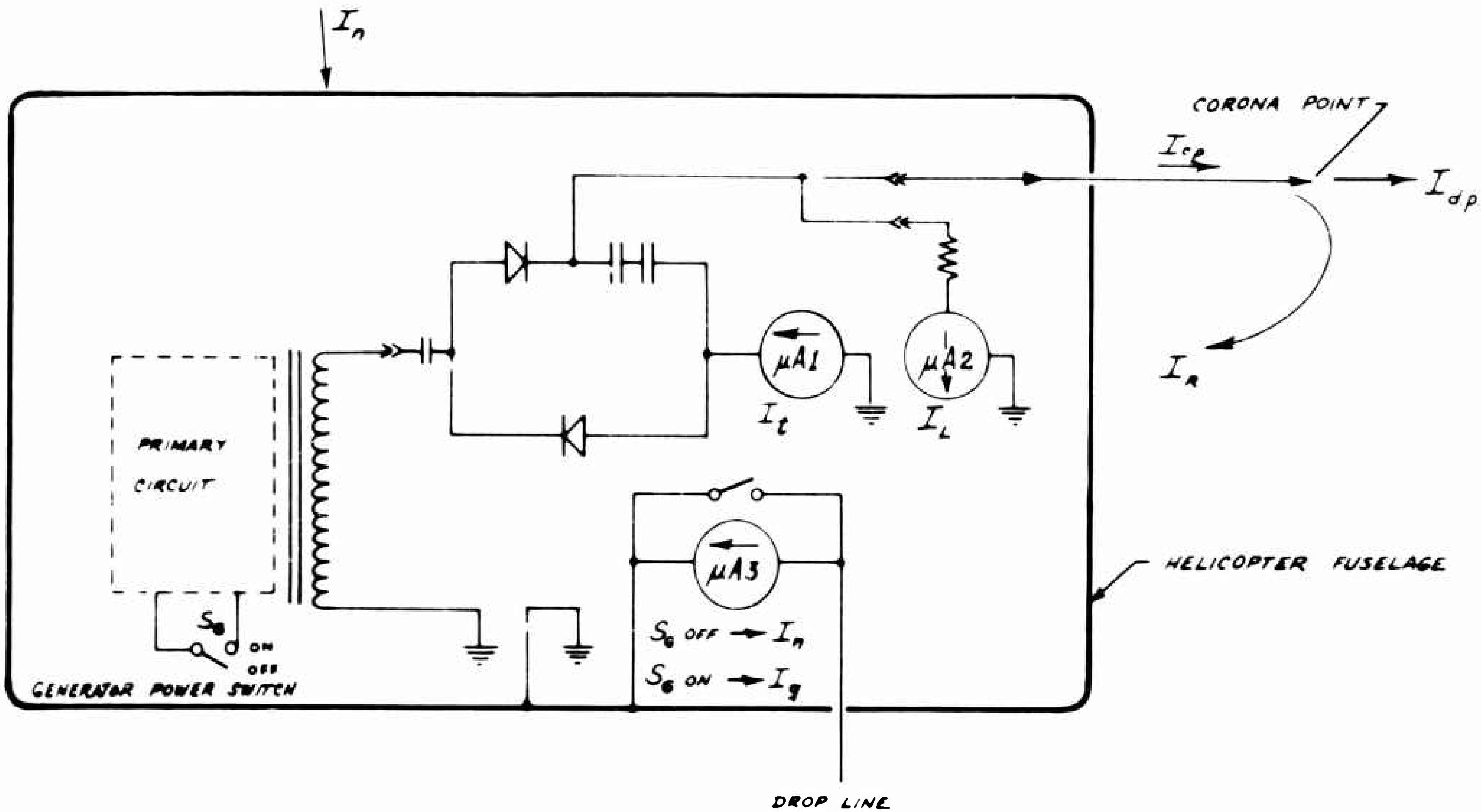

Procedure: 1. With S_G off, read the natural charging current I_n in $\mu A3$.

2. With S_G on, read: The ground current I_g in $\mu A3$
The total current I_t in $\mu A1$
The load current I_L in $\mu A2$

FIGURE 8: TEST CIRCUIT, CORONA POINT PERFORMANCE MEASUREMENT, KELLETT UNIT

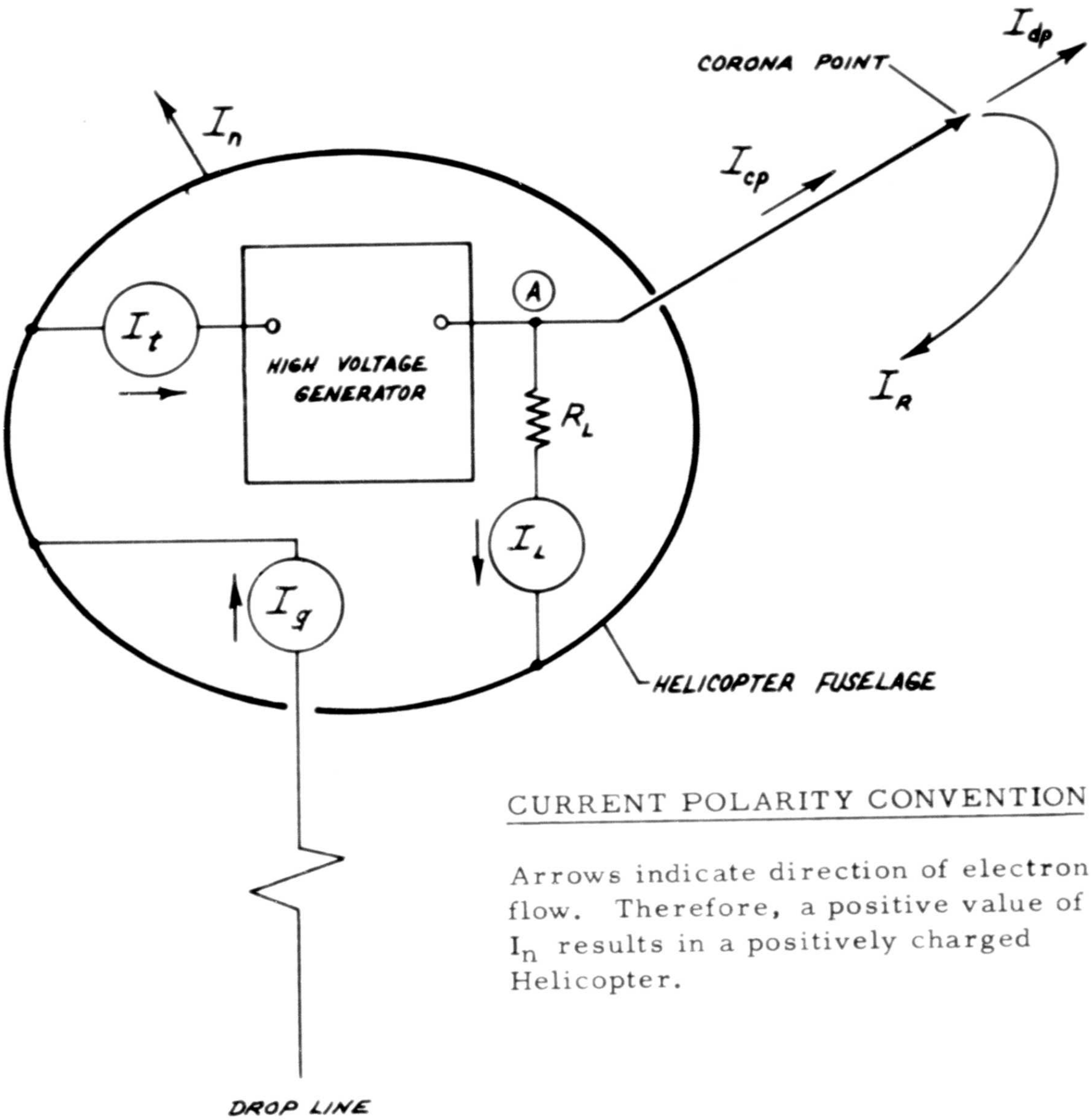

CURRENT POLARITY CONVENTION

Arrows indicate direction of electron flow. Therefore, a positive value of I_n results in a positively charged Helicopter.

FIGURE 9: TEST CIRCUIT, CORONA POINT PERFORMANCE MEASUREMENT, NJE UNIT OR SPELLMAN UNIT

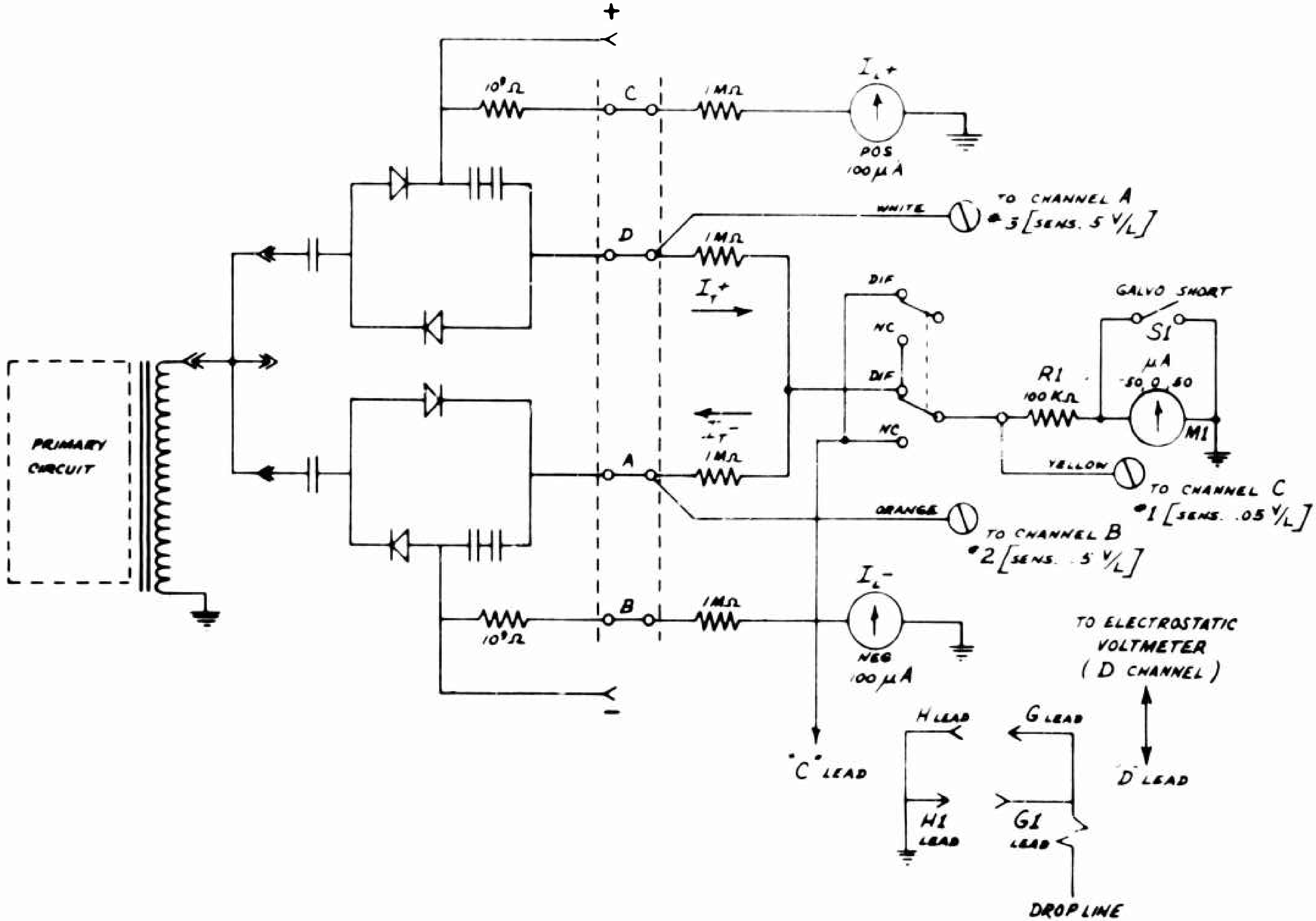

FIGURE 10: TEST CIRCUIT, DYNAMIC NEUTRALIZER PERFORMANCE MEASUREMENTS

Channel C — This channel was used in two different modes:

a. Natural charging current recording, and

b. Differential current between the positive and the negative high-voltage generators.

A switch on the control panel together with a high-voltage terminal interconnecting network were used to permit the test circuit to record in either mode.

To read natural charging current, the DIF-NC switch was thrown to NC (natural charging) and the following high voltage connections were made on the interconnecting network:

D lead to H lead
C lead to G lead
G1 lead to H1 lead, temporarily, as shown in Section D, "Experimental Procedure".

In this manner, the aircraft natural charging current was being released to ground through the M1 microammeter and the R1 resistor. The voltage drop at R1 was the input signal of the Channel C recording amplifier. When the dynamic neutralizer was turned on, Channel C was used to record the discharger differential current. The DIF-NC switch was turned to DIF (differential current) and the following connections were made in the interconnecting network:

D lead to G lead
C lead to H lead
G1 lead to H1 lead, temporarily, as shown in Section D, "Experimental Procedure". In this manner, the difference between the currents on the positive and negative generators was flowing through the microammeter M1 and the resistor, R1, and the voltage drop across R1 was used as the input of the Channel C recording amplifier.

Channel D — Helicopter voltage.

Leads G1 and H1, connected respectively to the drop line (ground) and the helicopter, were used to short-circuit the aircraft to ground when desired. In addition, these leads were used to limit the maximum aircraft voltage during the testing and to provide protection to the dividing head of the high-voltage electrometer. Figure 11 describes the construction of the high-voltage connector and shows how the air gap between the terminals was adjustable, providing a spark path when the aircraft voltage exceeded the dielectric strength of the air between the electrodes. This device was found to be very effective and simple to operate throughout the program.

3. Test Probes

Three (3) corona point lengths were used; 24, 36 and 48 inches, respectively, Reference Appendix I. The design of the nose-, tail- and engine-cowling-mounted corona points was such that the plastic insulating booms were interchangeable. The design of the engine exhaust point is different due to the temperature of the engine exhaust gases and the effect of the carbon deposits on the insulation of the probe. This corona point was designed to withstand temperatures up to 1200° Fahrenheit.

It should be noted that during the flight test program, a very noticeable amount of exhaust product deposits was formed on the main strut of the supporting structure of the exhaust corona point. However, the insulation characteristics of the structure were not affected by this contaminating deposit. A resistance insulation better than 10^{11} ohms at 50 kilovolts was measured for this contaminated structure.

4. Test Wire

High voltage wiring was installed in the helicopter airframe to connect the dischargers with the corona points. The wire used was nonshielded and was rated at 60 kilovolts DC. The wire was the Birnbach Radio Co., Inc., Catalog No. 7449. No failures were experienced on the high-voltage wiring. However, it was determined that a high level of static noise was generated by static charge accumulation and release in the external surface of the wire insulation.

D. EXPERIMENTAL PROCEDURE

1. Corona Point Performance Measurement

The measurement of the corona point performance was accomplished using the circuits of Figures 8 and 9. No

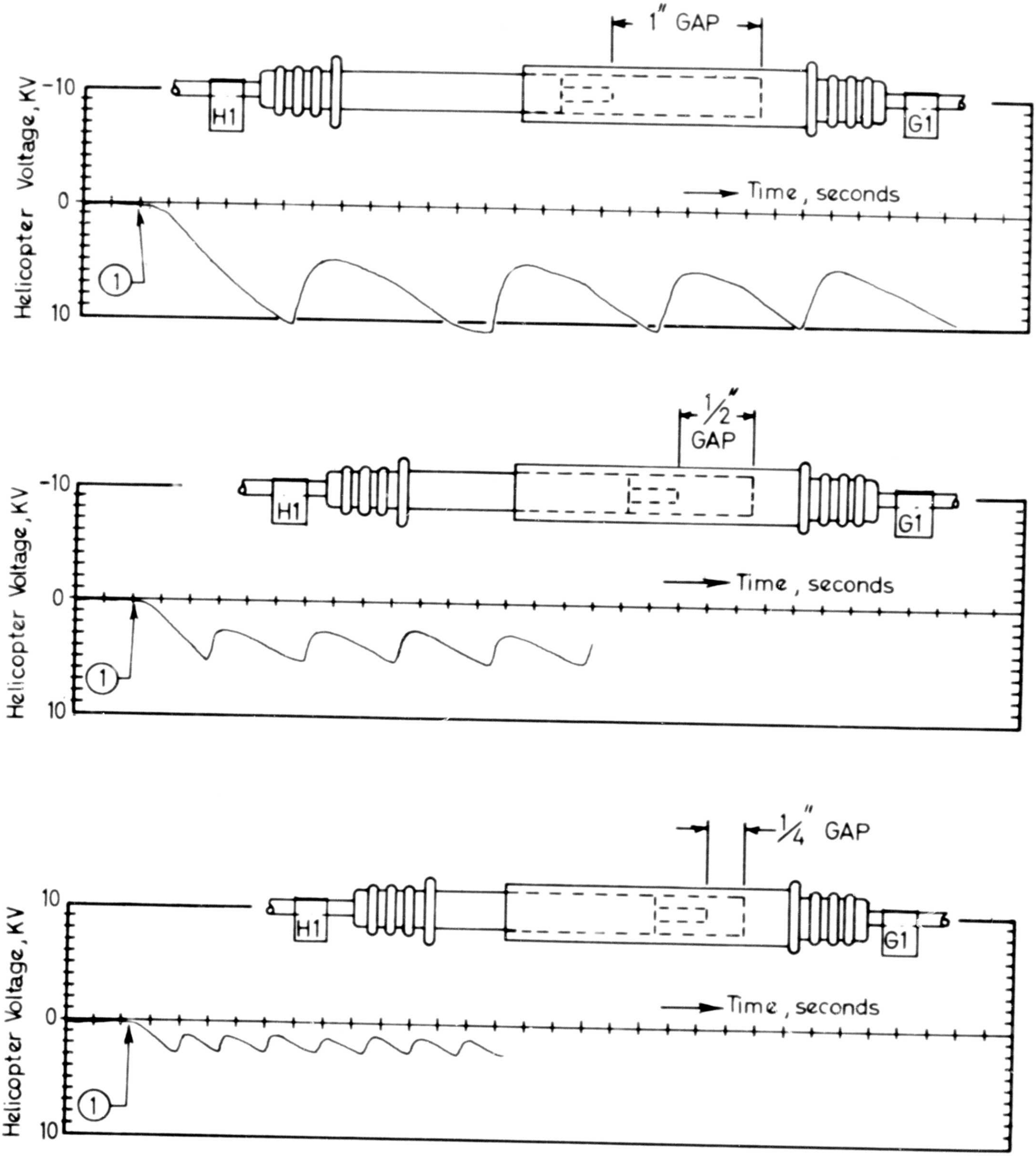

1: G1 lead separates from H1 lead

FIGURE 11: HIGH-VOLTAGE CONNECTOR, OPERATION ON AIRCRAFT VOLTAGE LIMITER (showing typical records obtained at different gaps).

time records were obtained for this measurement, due to the steady nature of all factors involved in the test.

The natural charging current existing prior to each test flight was measured and occasionally recorded. It has been experienced both in the present program as well as in previous experiences (References 1 and 3) that the level of natural charging current at the Edwards Air Force Base is in the order of 2 microamperes for an H-37 helicopter hovering at 25 feet. Hence, the reading of natural charging current obtained just prior to each corona current measurement may be considered constant during the duration (10-15 minutes) of each measuring period. Figure 12 reproduces an 85-second record of natural charging current. No natural charging current was read when the rotor of the helicopter was stationary.

The techniques used in the testing gave four microammeter readings for every test condition:

I_n Natural charging current

I_t Total current on the high-voltage generator

I_L Current on the load of the high-voltage generator

I_g Current between the helicopter and ground

These symbols are shown in Figure 9.

The relationships between the currents flowing in the test circuit can be determined by applying the first Kirchhoff law to the points indicated below.

a. Corona point tip $\quad I_{cp}-I_{dp}-I_R = 0 \quad (2)$

b. Point A, Fig. 9 $\quad I_t-I_L-I_{cp} = 0 \quad (3)$

c. Helicopter fuselage $\quad -I_n+I_g+I_L+I_R-I_t = 0 \quad (4)$

d. Ground-atmosphere $\quad I_{dp}+I_n-I_g = 0 \quad (5)$

The results of the testing performed in this program and shown in Table 2 shows that I_R is negligible when the helicopter is hovering.

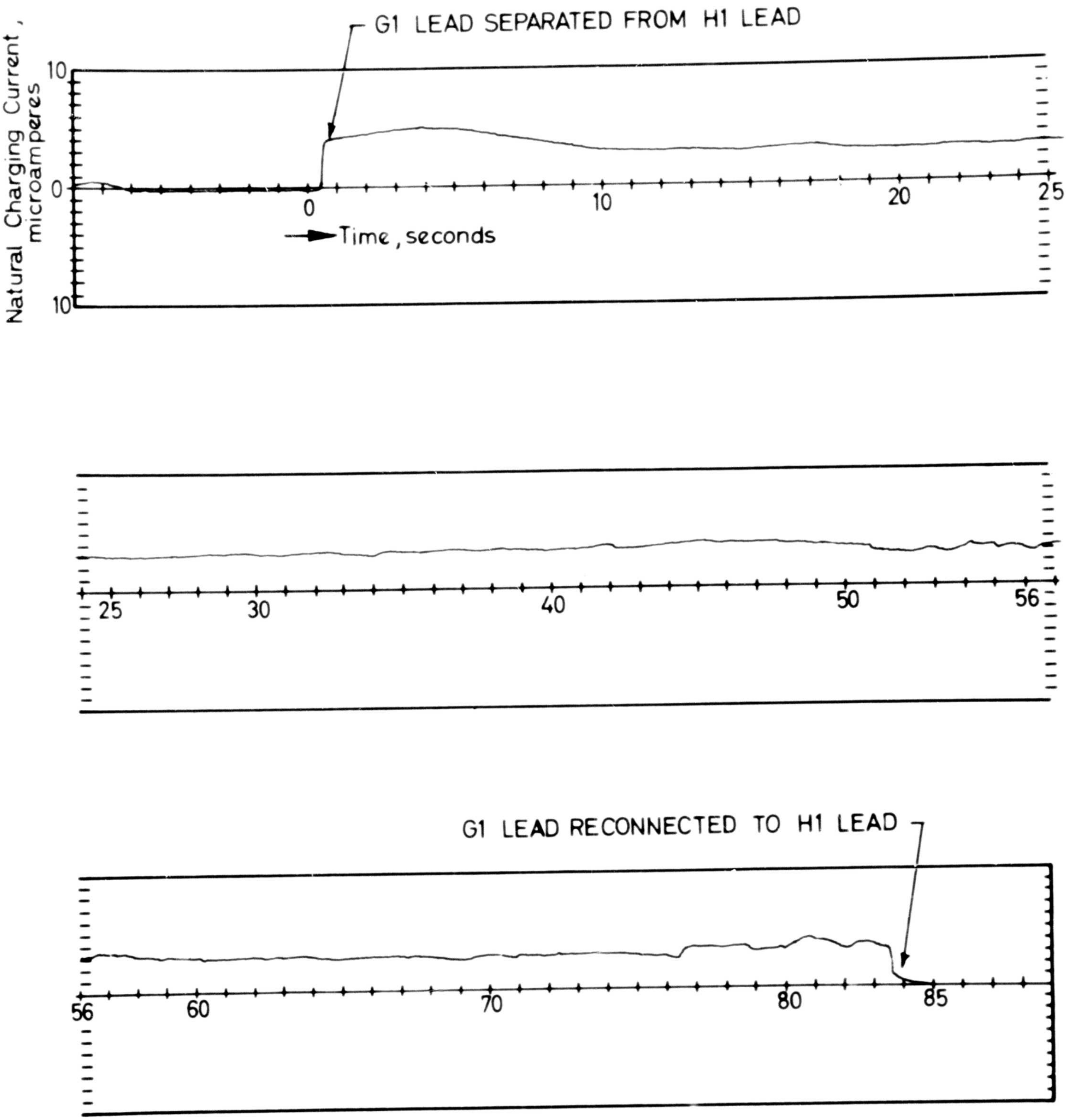

FIGURE 12: RECORD OF NATURAL CHARGING CURRENT

TABLE 2

CORONA POINT PERFORMANCE

HOVERING FLIGHT, 25 FT. ALTITUDE

(See Figures 8 & 9 for Notation; Current in Microamperes)

Corona Point Configuration Code	Measured Data				Derived Data		
	I_n	$I_L = -KV$	I_g	I_t	$I_{cp} = I_t - I_L$ Eq. (3)	$I_{dp} = -I_n + I_g$ Eq. (5)	$I_R = I_t + I_n - I_g - I_L$ Eq. (2) or (4)
LE2	+2	-25	- 7	-35	-10	- 9	-1
	+2	-30	- 8.5	-	-	-10.5	-
	+2	-40	-17	-60	-20	-19	-1
	+2	-50	-21.5	-	-	-23.5	-
	+2	-60	-27	-	-	-29	-
RE2	+2	-30	- 9.5	-	-	-11.5	-
	+2	-50	-21.5	-	-	-23.5	-
	+2	-60	-26	-	-	-28	-
LE3	+2	-30	- 7	-	-	- 9	-
	+2	-50	-19	-	-	-21	-
	+2	-60	-23	-	-	-25	-
RE3	+2	-30	- 7	-	-	- 9	-
	+2	-50	-18	-	-	-20	-
	+2	-60	-21.5	-	-	-23.5	-
LE4	+2	-24	- 5	-31	- 7	- 7	0
	+2	-30	- 6	-	-	- 8	-
	+2	-50	-15	-	-	-17	-
	+2	-60	-17	-	-	-19	-
RE4	+2	-30	- 6	-	-	- 8	-
	+2	-50	-15	-	-	-17	-
	+2	-60	-18	-	-	-20	-
LT2	+2	-30	- 6	-	-	- 8	-
	+2	-50	-16	-	-	-18	-
	+2	-60	-21	-	-	-23	-

TABLE 2 (CONTINUED)

Corona Point Configuration Code	(See Figures 8 & 9 for Notation, Current in Microamperes) Measured Data I_n	$I_L = -KV$	I_g	I_t	Derived Data $I_{cp} = I_t - I_L$ Eq. (3)	$I_{dp} = -I_n + I_g$ Eq. (5)	$I_R = I_t + I_n - I_g - I_L$ Eq. (2) or (4)
RT2	+2	-30	- 9	-	-	-11	-
	+2	-50	- 7	-	-	-19	-
	+2	-60	-22	-	-	-24	-
LT3	+2	-22	- 6	-30	- 8	- 8	0
	+2	-30	- 7	-	-	- 9	-
	+2	-50	-14	-	-	-16	-
	+2	-60	-21	-	-	-23	-
RT3	+2	-22	- 5	-30	- 8	- 7	- 1
	+2	-30	- 8	-	-	-10	-
	+2	-50	-18	-	-	-20	-
	+2	-60	-23	-	-	-25	-
LT4	+2	-26	- 7	-37	-11	- 9	- 2
	+2	-30	- 6	-	-	- 8	-
	+2	-40	-15	-58	-18	-17	- 1
	+2	-50	-15	-	-	-17	-
	+2	-60	-20	-	-	-22	-
RT4	+2	-26	- 5	-33	- 7	- 7	0
	+2	-30	- 8	-	-	-10	-
	+2	-40	-13	-55	-15	-15	0
	+2	-50	-15	-	-	-17	-
	+2	-60	-22	-	-	-24	-
LN4	+2	-26	0	-28	- 2	- 2	0
RN4	+2	-26	0	-28	- 2	- 2	0
LC4	+2	-26	- 1	-29	- 3	- 3	0
	+2	-30	- 2	-	-	- 4	-
	+2	-50	- 5	-	-	- 7	-
RC4	+2	-26	- 1	-29	- 3	- 3	0

The operating voltage of the Kellett-built generator was measured by using the load current reading I_L. The load resistance was a 10^9-ohms precision (2%) resistor. Hence, the voltage-to-current ratio in this load was one kilovolt per microampere. In this manner, the voltage in kilovolts on the generator was equal to the load current, expressed in microamperes.

2. Dynamic Neutralizer Performance Measurements

The measurement of the performance of the dynamic neutralizer static electricity discharger was made, as explained previously, by measuring and recording the voltage to ground of the test aircraft with and without the unit in operation. An air gap voltage limiter (Figure 11) protected the voltmeter input circuit from voltages exceeding its maximum rated value. Simultaneously, with the aircraft voltage, the differential current flowing through the discharging unit was also recorded. This record was made in order to provide a redundant check of the operation of the instrumentation, because the differential current must be equal to the natural charging current (recorded prior to each dynamic neutralizer test run) once the aircraft voltage reaches a steady state value.

Figure 13 shows a typical record of the performance of the dynamic neutralizer. As indicated in the record, the aircraft was first grounded by connecting the terminals, G1 and H1 (see electrical diagram in Figure 11). This, together with the closing of the switch, S1, protected the microammeter, M1, and amplifier input circuits against the high-voltage transient originated at the instant at which the drop line touched the ground target.

The natural charging current was first recorded obtaining records as shown in Figure 12. Then the aircraft was grounded again by joining the connectors, G1 to H1, the DIF-NC switch was turned to DIF, and the dynamic neutralizer was left OFF for some time after the restart of the recorder. Under these conditions (grounded aircraft and discharger OFF), the zero of the two channels, C and D, was clearly established on the records. Then, with the discharger still OFF, the aircraft was ungrounded by opening G1 from H1. As shown in the sample record (Figure 13), the aircraft voltage started rising immediately, until a value determined by the G1-H1 air gap dielectric strength. At this value, a spark was produced in

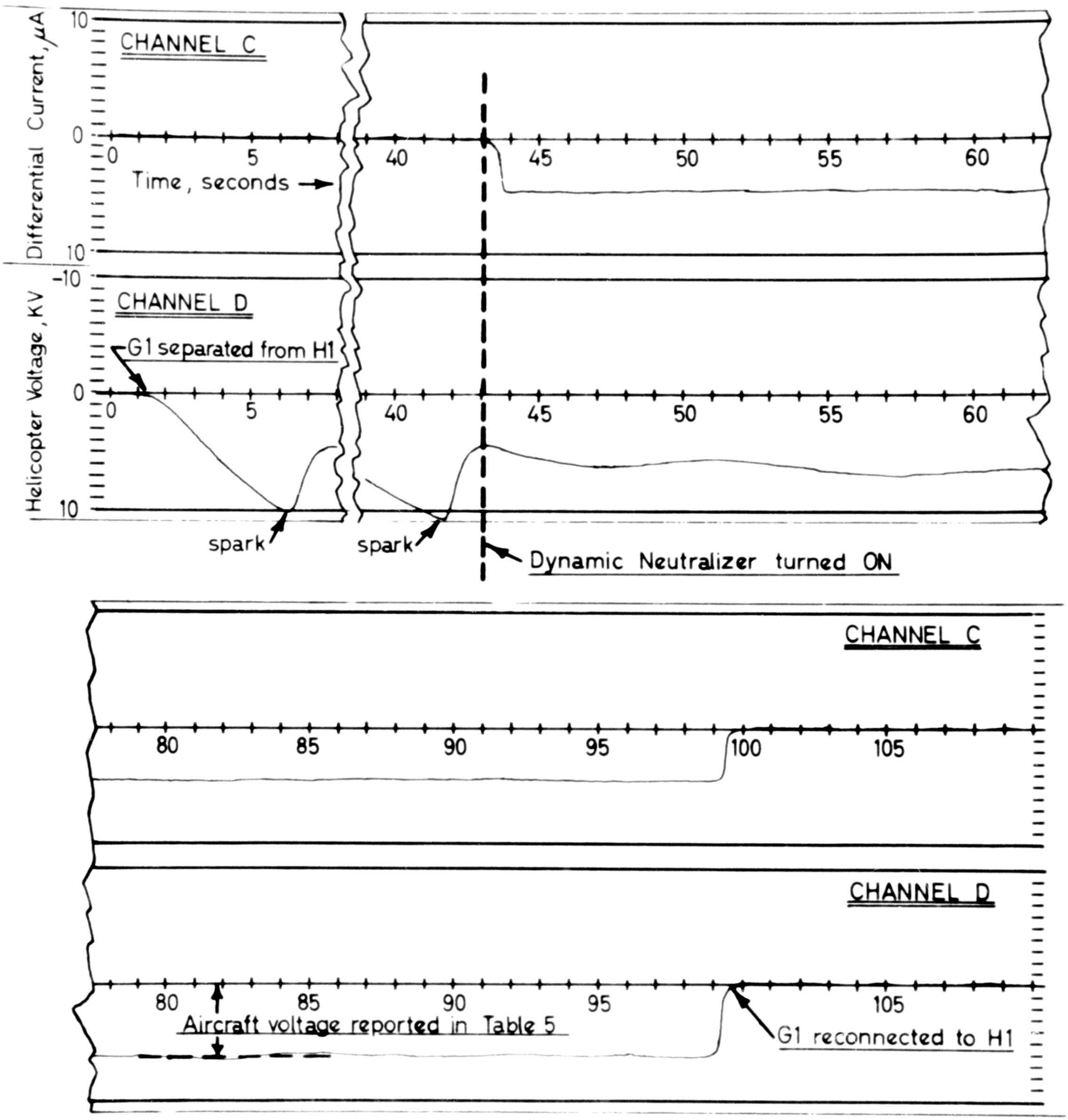

FIGURE 13: RECORD OF DYNAMIC NEUTRALIZER OPERATION

the gap, and a major portion of the aircraft accumulated charge was released to ground through the spark, bringing the aircraft voltage down to a few thousand volts. After experiencing several sparks, the dynamic neutralizer was turned ON. Now the aircraft voltage rose more slowly, and an equilibrium voltage was reached after a number of seconds. At the same time, Channel C recorded the differential current flowing through the unit. This differential current was substantially equal to the natural charging current recorded in the first part of the test.

In addition to these records, readings were made both in the natural charging - differential current microammeter and in the high-voltage electrometer. In some tests, and due to operational problems, time records were omitted and only microammeter readings were recorded. It should be noted that excellent agreement was found between oscillograph records and the microammeter readings made throughout the test program.

E. EVALUATION OF THE TEST DATA

1. Data Presentation

Tables 2 through 5 and Figures 14 through 19 present the results of the measurements performed during this test program. In order to identify the corona point configuration used in each test, a coded designation has been assigned to each configuration. The code consists of two letters and a digit. The following chart explains the code.

Configuration Code - EXAMPLE

R T 3

First Letter

R. Right Hand Side Probe (aircraft starboard)

L. Left Hand Side Probe (aircraft port)

Second Letter

T Tail Probe
E Exhaust Probe
C Cowling Probe
N Nose Probe

Digit

4. 4' long corona point

3. 3' long corona point

2. 2' long corona point

Refer to Appendix I to detailed drawings of corona point probes. Refer to Figure 3 to obtain detailed locations of probes.

TABLE 3

CORONA POINT PERFORMANCE MEASUREMENTS

RAMP TESTS ($I_n = 0$)

See Figure 9 for Symbols
Current in Microamperes

Corona Point Configuration Code	Measured Data $I_L = KV$	$I_g = I_{dp}$ Eq.(5)	I_t	Derived Data $I_{cp} = I_t - I_L$ Eq.(3)	$I_R = I_t - I_L - I_g$ Eq. (4)	
RT3	26	.8	30	4	3.2	Wind approximately 20 knots from 45° relative bearing.
LT3	26	1	30	4	3	
RN4	26	.4	30	4	3.6	
LN4	26	1.5	31	5	3.5	
RC4	26	1.8	31	5	3.2	
LC4	26	3	31	5	2	
LE4	26	.8	30	4	3.8	
RT4	25	3.5	30	5	1.5	Wind approximately 12 to 20 knots, 10° relative bearing.
RT4	40	4.5	48	8	3.5	
RT4	46	5	-	-	-	
LT4	26	2.5	31	5	2.5	
LT4	40	4	48	8	4	
LT4	47	5	-	-	-	
LE2	25	1.7	30	5	3.3	
LE2	40	4.5	48	8	3.5	
LE2	46	5	-	-	-	

TABLE 4

CORONA POINT PERFORMANCE MEASUREMENTS

MEASUREMENTS INSIDE THE HANGAR

AT ZERO AIR SPEED
($I_n = 0$)

Corona Point Configuration Code	See Figure 9 for Symbols Current in Microamperes I_L-KV	$I_{dp}=I_g$ Eq. (5)
RT3	+25	+ .5
LT3	-25	- .5
RN4	-25	-1
LN4	+25	+1
LC4	+25	+1
LC4	+10	Not readable
LC4	+20	+ .25
LC4	+26	+1.5
Portable, Conf. A (See below)	+26	+1
Portable, Conf. B (See below)	+26	Not readable
Portable, Conf. C	+26	+6

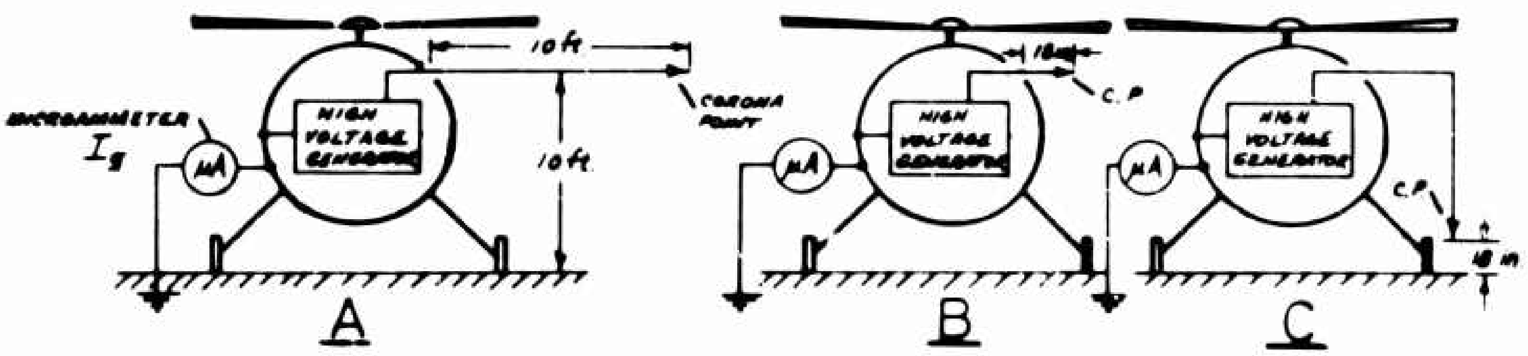

TABLE 5

DYNAMIC NEUTRALIZER PERFORMANCE MEASUREMENTS

Date	Probe Code	Natural Charge, Microamperes	Generator Voltage, Kilovolts	Helicopter Voltage, Kilovolts	
5/11/62	T3	4-5	±40	10	
5/17/62	T4	4-5	±40	8-10	Kellett
5/17/62	T4	4-5	±46	6-10	Unit
5/18/62	T4	4	-40,+44	5-7	
5/18/62	T4	4	-22,+26	6.5-9	
5/25/62	T4	2	50	+5	
5/25/62	T4	2	60	+3	
5/25/62	E-2	2	50	+4,+6	
5/25/62	E-2	2	60	+7,+10	
5/25/62	T3	2	50	+6,+6.5	Spellman-
5/25/62	T3	2	60	+3.5,+4	NJE
5/25/62	E-3	2	50	±5	Combina-
5/25/62	E-3	2	60	+3,+3.2	tion
5/25/62	T2	3	50	+8,+10	
5/25/62	T2	3	60	+5,-3	
5/25/62	E-4	3	50	+6,+6.5	
5/25/62	E-4	3	60	+3,+4	

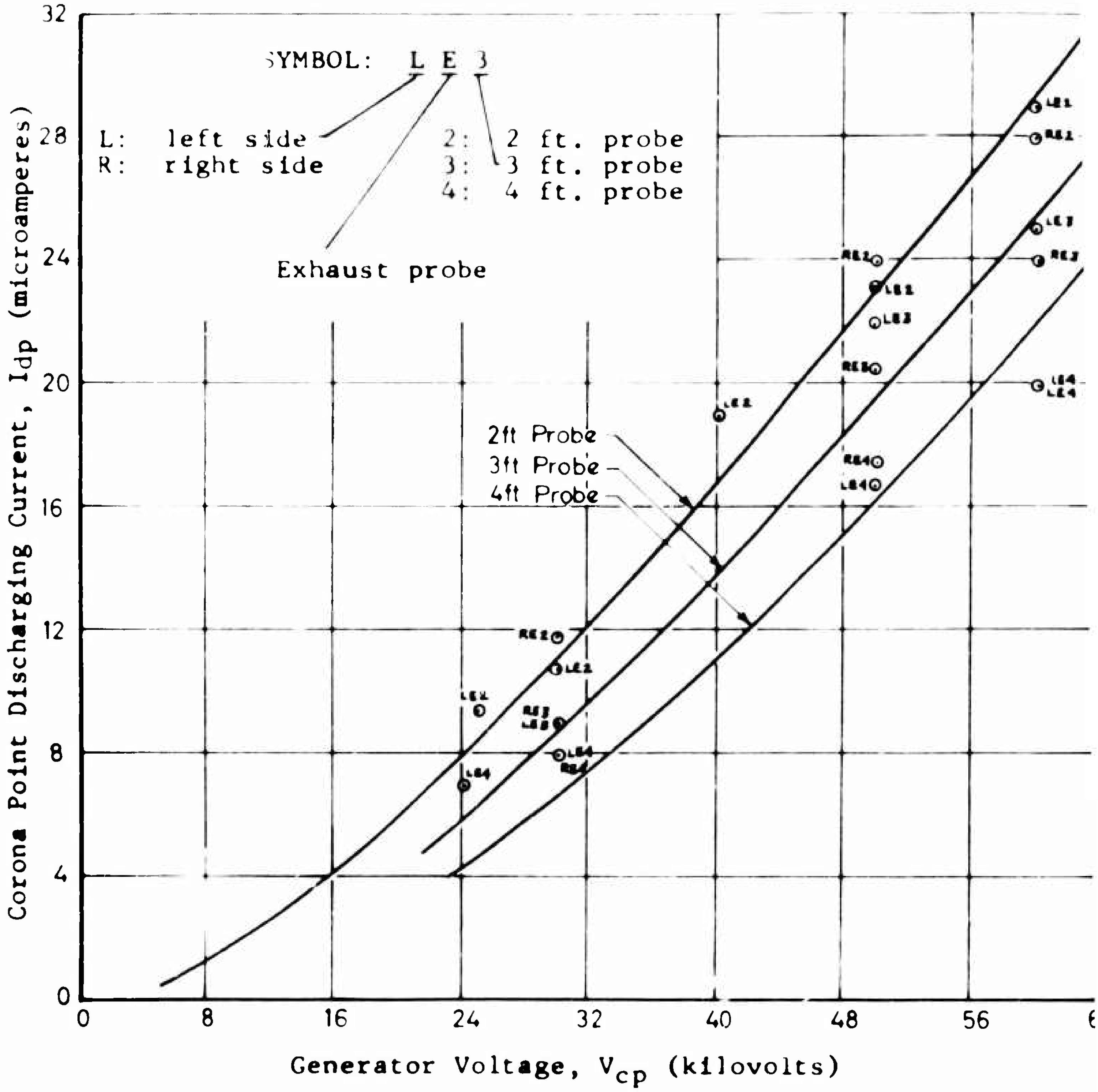

FIGURE 14: CORONA POINT PERFORMANCE, EXHAUST CORONA POINTS

NOTES: 1. Readings at 30, 50, and 60 KV taken in same flight. Observe the consistent RT & LT.

2. No consistency on the behavior of 4, 3, and 2 points.

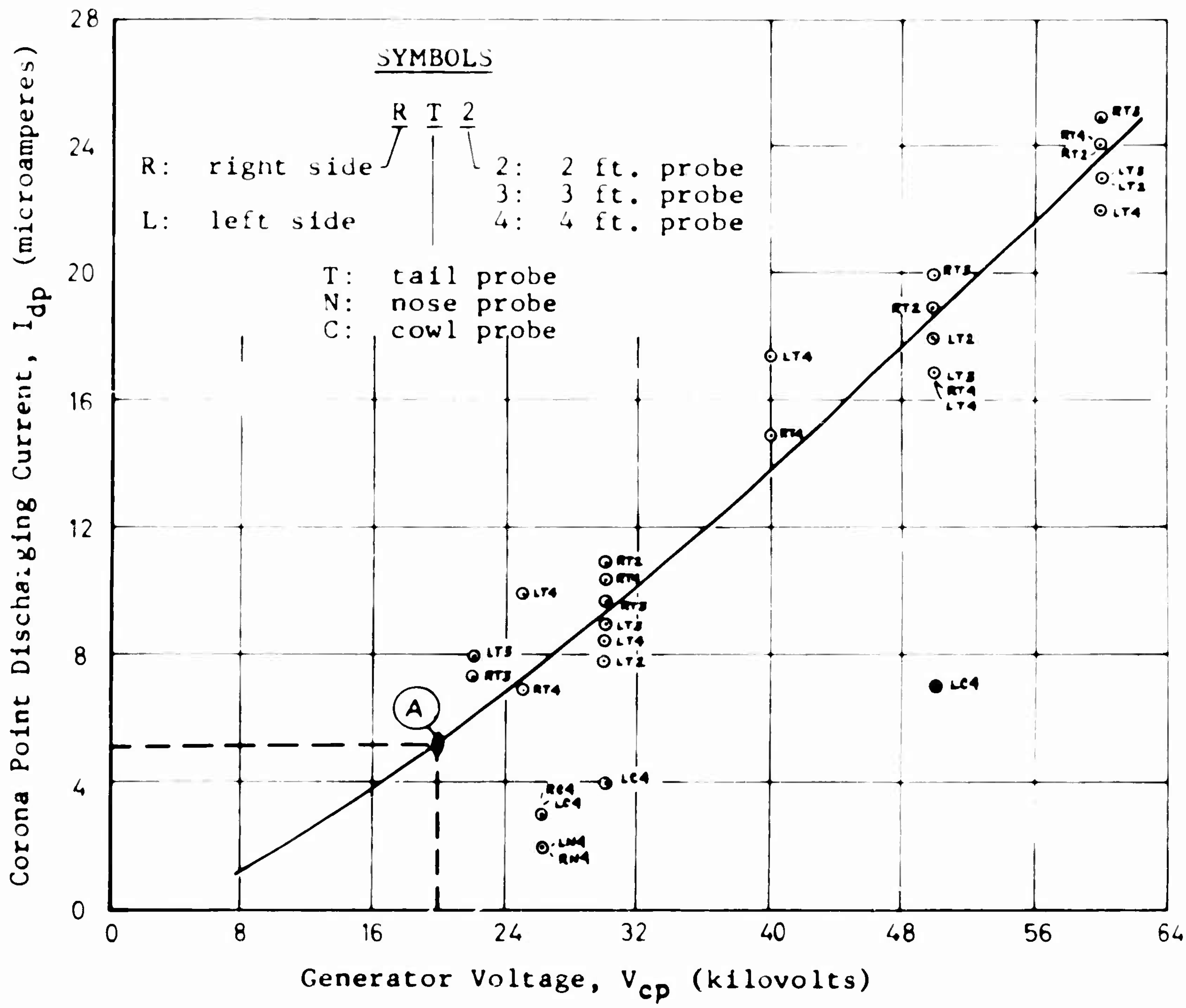

FIGURE 15: CORONA POINT PERFORMANCE, TAIL, NOSE AND COWL CORONA POINTS

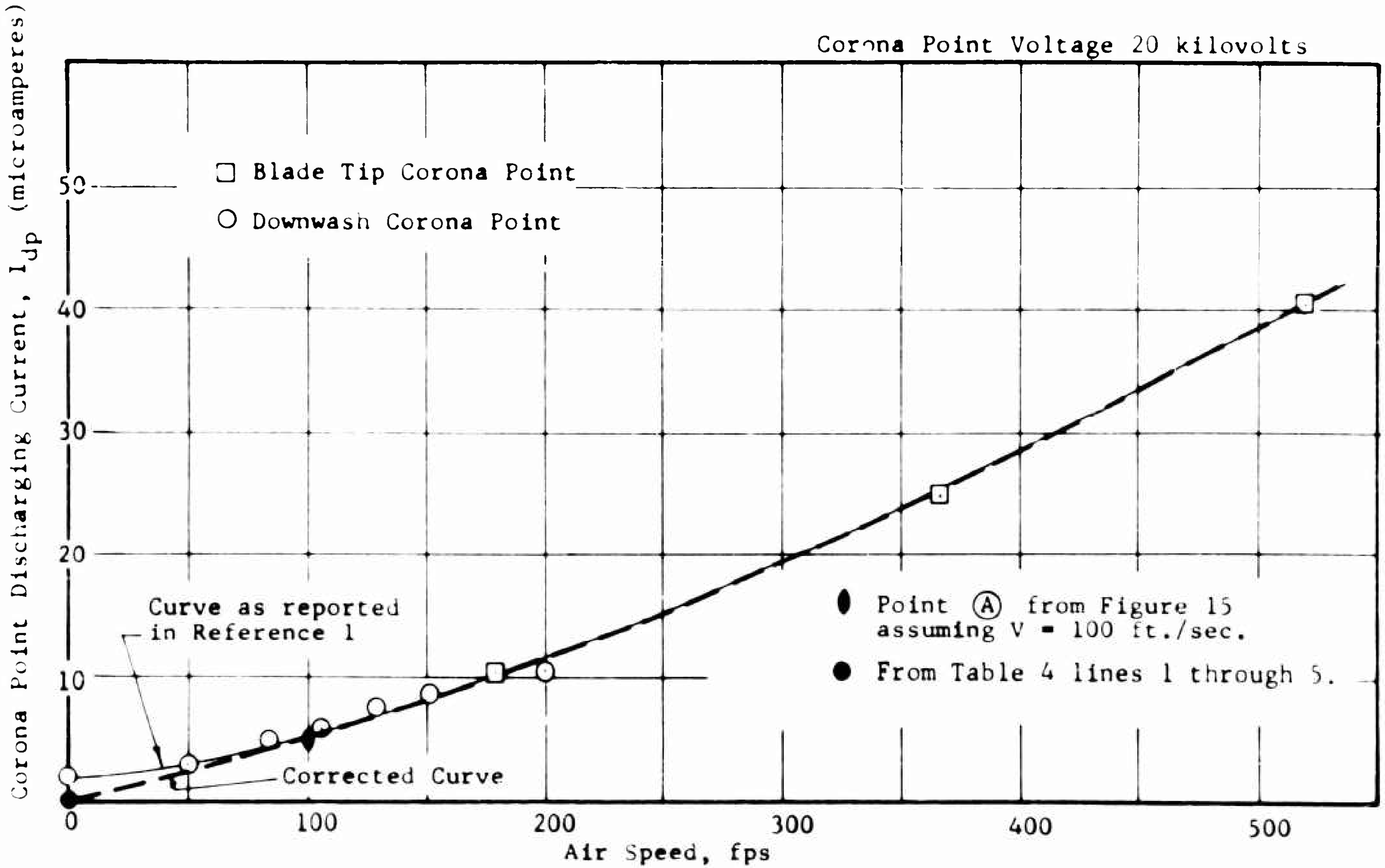

FIGURE 16: CORONA POINT PERFORMANCE VS. AIR SPEED CORRECTED CURVE

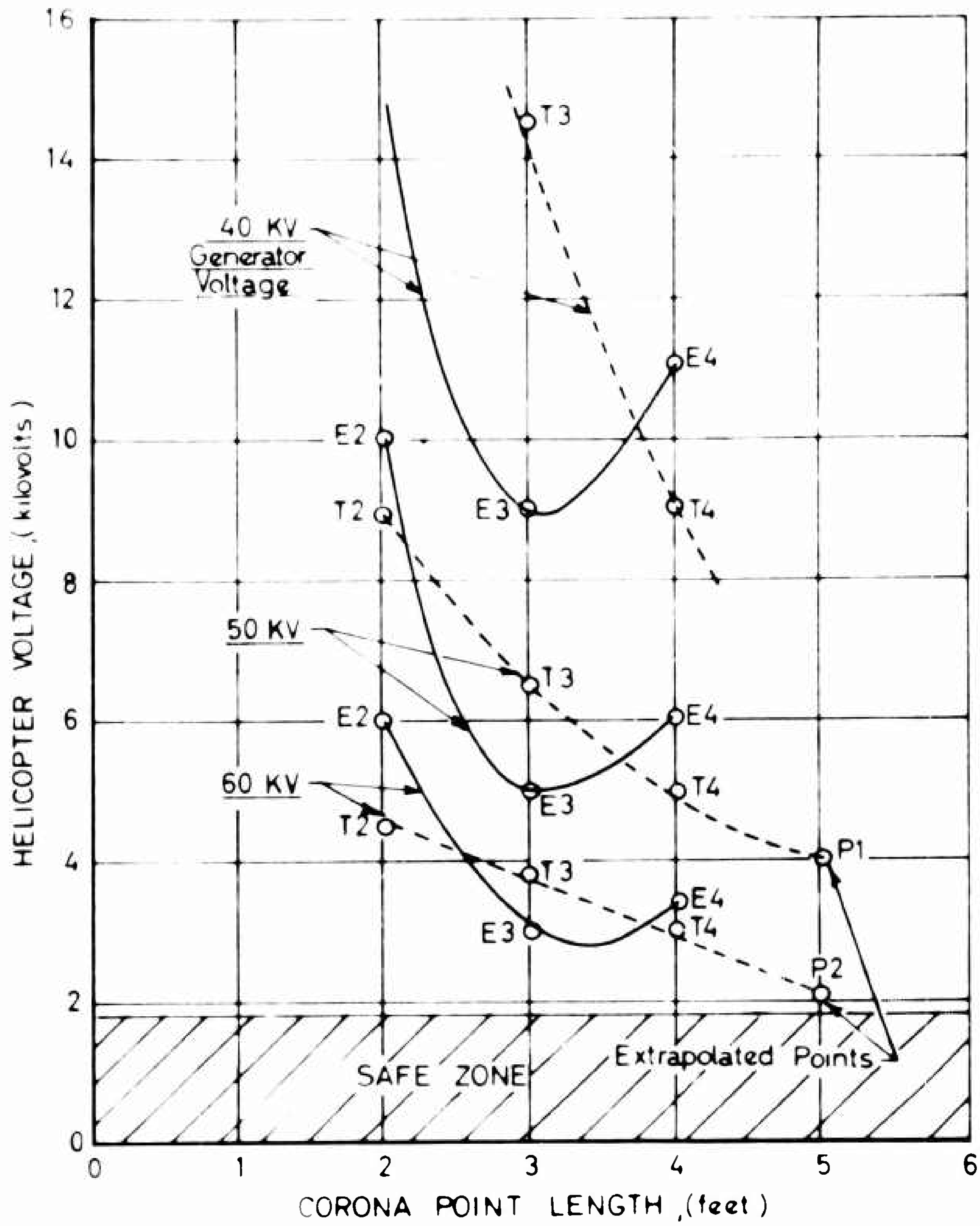

FIGURE 17: DYNAMIC NEUTRALIZER PERFORMANCE, TAIL AND EXHAUST CORONA POINTS

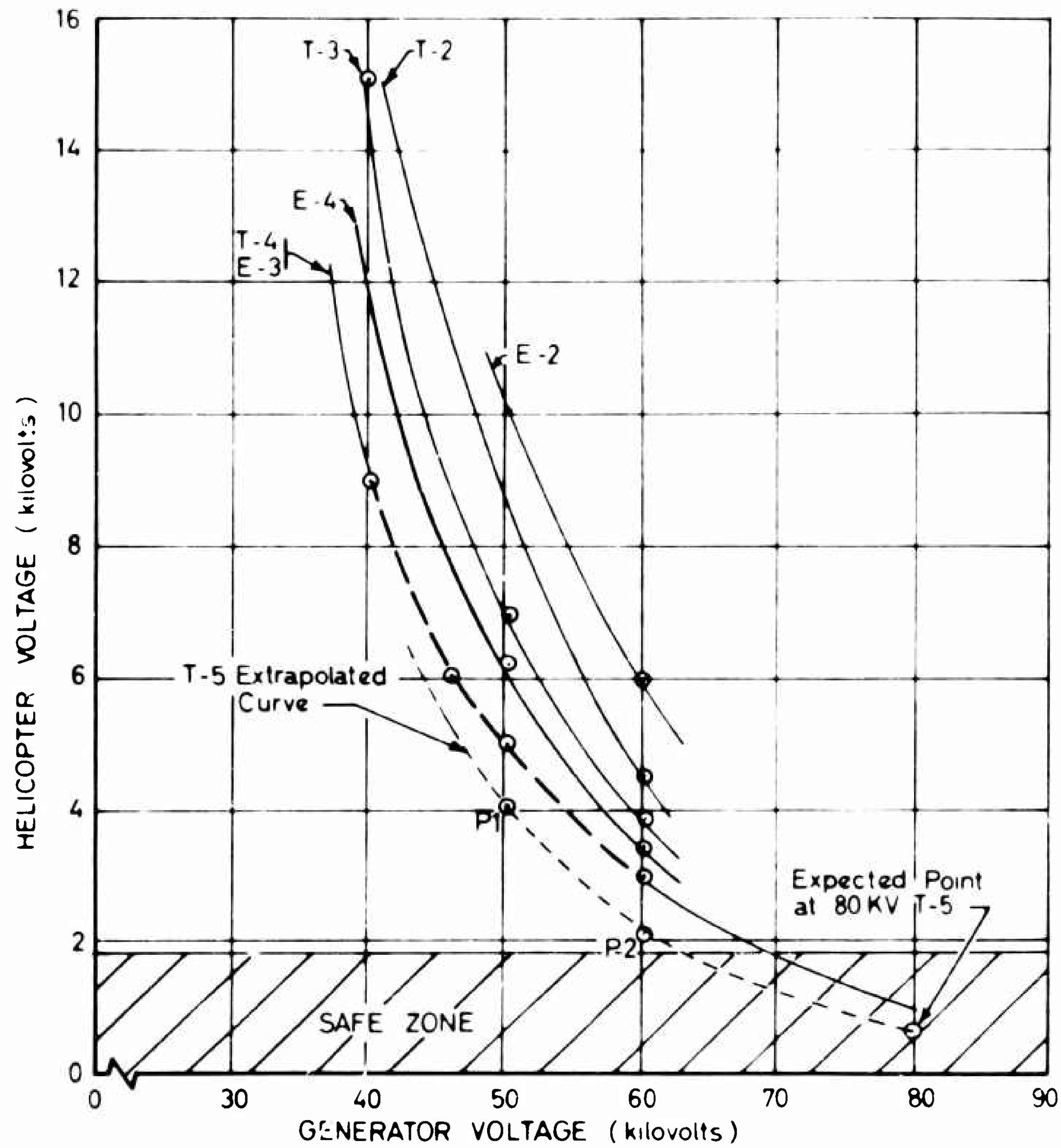

FIGURE 18: DYNAMIC NEUTRALIZER PERFORMANCE, GENERATOR VOLTAGE VS. HELICOPTER VOLTAGE PLOT

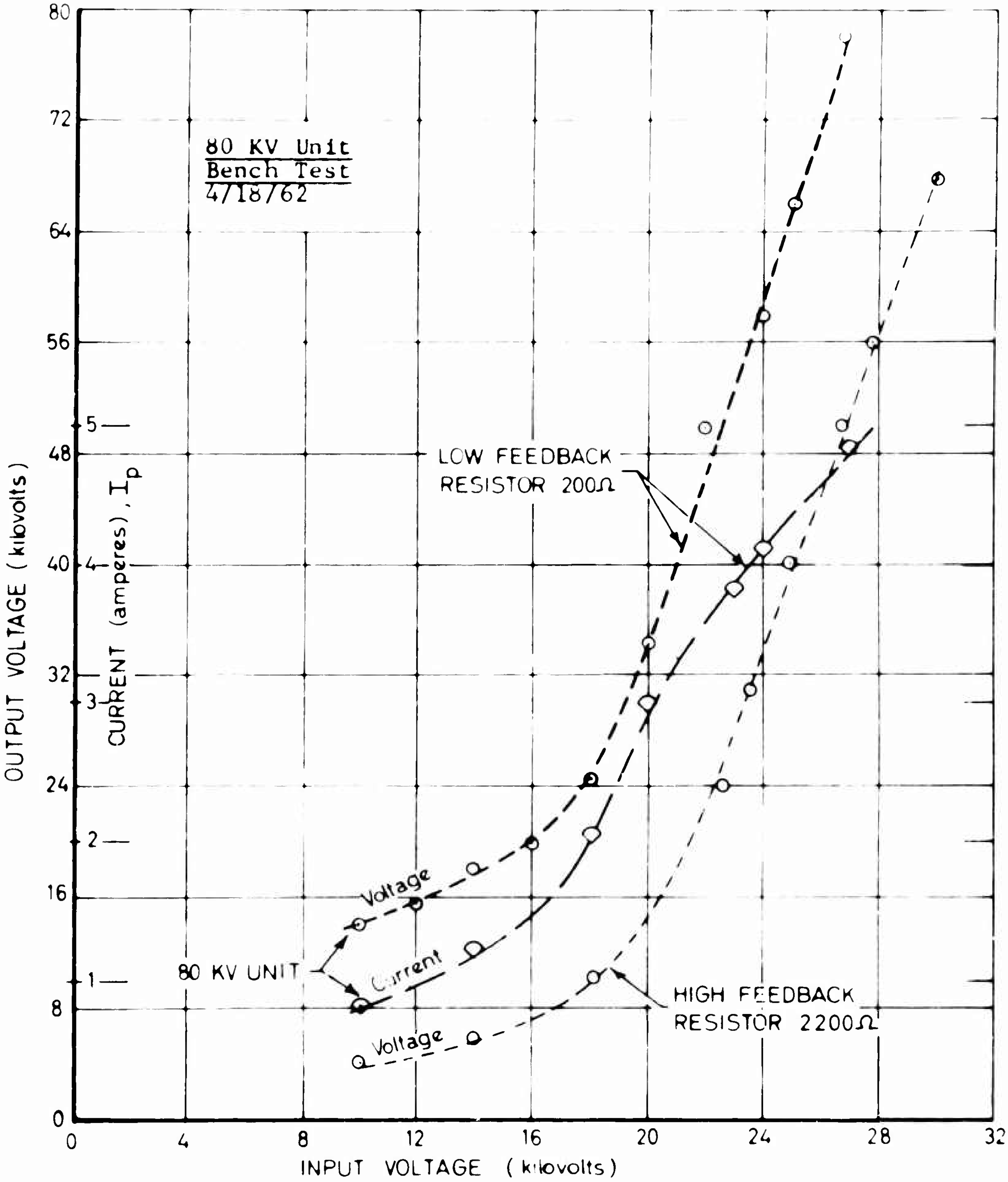

FIGURE 19: DYNAMIC NEUTRALIZER VOLTAGE OUTPUT VS. VOLTAGE INPUT

2. Corona Point Performance

Table 2 shows the results of the corona point performance measurements in hovering flight at 25 feet. As seen from Table 2, the natural charging current was 2 microamperes during all tests. The load current, I_L, was varied up to an equivalent generator voltage of 60 kilovolts and readings were made, for the various corona point configurations, of the helicopter-to-ground current, I_g, and the total generator current, I_t. The derived corona point discharging current, I_{dp}, data is plotted for the exhaust probes in Figure 14 and for the tail-mounted probes in Figure 15. Some data have also been obtained with the corona points mounted on the nose and cowling, and these data are also shown on Figure 15. As noted, the performance of the nose- and cowl-mounted probes was greatly inferior to that of the other probes; hence, the major part of the testing was concerned with the tail and exhaust probes. The limited performance of the nose and cowl probes is attributed to the lower air speed at these locations.

The data shown in Figure 15 also indicate that the performance of the tail-mounted probes is not affected in a consistent manner by the probe length. On the other hand, as seen in Figure 14, the performance of the exhaust probes is clearly affected by probe length. The performance of all probes tested increases almost linearly with generator voltage. The effect of air speed is clearly shown in Figure 14 since an increase of corona point length implies a decrease of the exhaust gas speed due to the stream expansion.

The corona point that resulted in the highest performance is the 2-foot-long exhaust- mounted point. For this point, a current of 29 microamperes at 60 kilovolts was recorded.

Table 3 presents the corona point performance data obtained for the tests on the ramp, and Table 4 presents the data obtained in the hangar. These tests indicated that the data presented in Figure 13 of Reference 1 are incorrect in the low speed range. The corrected variation of corona point performance with air speed is presented in Figure 16. It is noted that the corona point current is practically zero for zero air speed.

It may be noted from Table 3 that the current output of geometrically symmetric probes is not identical for the tests performed on the ramp. In particular, it is seen from the data that the current flowing from the probes mounted on the port side of the aircraft exceeds that flowing from the probes mounted on the starboard side. The explanation for this phenomenon is concerned with the relative wind. The tests were performed with the wind flowing from the front to starboard side of the helicopter. The resulting air flow entrains charged particles emerging from the probes. Because of geometric considerations, it appears, therefore, that some of these particles emerging from the right probe are blown toward the helicopter skin and hence recaptures by the aircraft. On the other hand, the air flow assists the charged particles emerging from the left probes to escape from the helicopter. As explained previously, the net discharging current of an active corona point is the difference between the current flowing from the probe and the current recaptured by the helicopter. For these tests the rotor blades were stationary and the engine was stopped. Hence, no natural charging current was generated. As such, the difference of performance of the two probes is a direct indication of the importance of the probe location and the air flow relative to the aircraft.

It is of interest in this instance to examine the probe performance data in the hovering flight tests, presented in Table 2 and Figures 14 and 15. It may be noted, that there is no consistency in the difference of performance between the left and right probes located in the exhaust or on the fuselage tail. An explanation for this behavior is obtained again by considering the local air flow. In the hovering flight condition, the remote wind is only a small part of the resultant air flow. In fact, the rotor downwash for the tail probes and the exhaust velocity for the exhaust probes are the determining factors in the performance of the probes. The unsteady nature of these velocities accounts for the variation of the test data.

Another item of interest concerns the magnitude of the current that is recaptured by the aircraft after being emitted from the corona points, I_R . The corona point performance data obtained with a hovering helicopter, as shown in Table 2, indicate that almost all of the current flowing through the corona point is blown into the atmosphere. This is substantiated by the low value attained by I_R through Table 2. However, in the ramp measurements listed in Table 3, it can be seen that the current returning to the aircraft, I_R, accounts for the larger part of the total current, I_{cp}, flowing through the corona points.

3. Dynamic Neutralizer Performance

Table 5 gives the results of the measurements of the dynamic neutralizer performance in a chronological order.

The performance of the dynamic neutralizer using exhaust and tail corona points is shown in Figure 17 as a plot of the helicopter voltage against the corona point length, using as fixed parameters the generator voltage and the corona point configuration. Figure 17 includes three extrapolated points which will be discussed subsequently.

Figure 18 is a different presentation of the data of Table 5, where the helicopter voltage is plotted against the generator voltage, using the corona point configuration as constant parameter. In addition, the points extrapolated in Figure 17 have also been presented in Figure 18. A further extrapolation has been performed up to a generator voltage of 80 kilovolts.

Figure 19 is a plot of the dynamic neutralizer voltage output versus voltage input for two different feedback resistance values. The data in Figure 19 were obtained during the laboratory testing of the unit. This figure is included herein to provide data concerning the power requirements of an eventual operational dynamic neutralizer electrostatic discharging system.

An evaluation of these test data on the performance of the dynamic neutralizer shows:

a. The dynamic neutralizer within the range of generator voltage (0-60 kilovolts) and probe size (2 to 4 feet) used in the present program reduces the electrostatic energy of the H-37 aircraft down to a minimum value of 3.4 millijoules under the natural charging conditions prevailing at Edwards Air Force Base (2-4 microamperes). This value is larger than the maximum energy level considered satisfactory according to References 1 and 3.

b. The performance of the dynamic neutralizer depends on three different factors:

(1) The operating voltage
(2) The air speed at the corona point
(3) The probe geometry and its location relative to the aircraft geometry.

This conclusion agrees with the theory and with the findings reported in Reference 1.

c. As seen from Figure 17, the system performance, using tail-mounted corona points, improves steadily when the corona points are placed at greater distances from the helicopter skin. It is also noted that this trend is different for the exhaust-mounted probes.

This fact may be explained by noting that, with the tail corona points, the air speed does not change appreciably as a function of the length of the probe. Hence, the only factor which determines performance changes is the smaller influence of the aircraft field on the longest corona point, which results in larger differential currents between the positive and negative corona points.

On the contrary, in the exhaust installation, the increased separation is overcompensated by the decrease in air speed due to the exhaust gas stream expansion. This explains why the exhaust configuration possesses an optimum performance for a probe of about 3-foot length.

d. An extrapolation is carried out to determine the possible performance of the dynamic neutralizer under higher voltages and with longer probes. Referring first to Figure 17, the points P1 and P2 are obtained extrapolating the probe length up to 5 feet. Next, P1 and P2 are transferred to Figure 18. Extrapolating now further the curve T5 so obtained, up to an operating voltage of 80 kilovolts, it is estimated that an 80-kilovolt system, using 5-foot-long corona points, would reduce the helicopter voltage to a value below 1 kilovolt. This voltage corresponds to an energy level of 0.375 millijoule, which falls within the limit of satisfactory operation. It should be noted, however, that these data were obtained for the range of natural charging current existing at the test site.

e. The effect of the natural charging current on the sensitivity of the dynamic neutralizer has not been investigated in the present program. Natural charging current levels ranging from 2 to 5 microamperes were encountered and recorded as shown in Table 5. However, the data obtained do not lend themselves to determining the effect of the magnitude of natural charging current on the performance of the dynamic neutralizer. This fact may be explained as being due to the relatively small magnitude of all natural charging currents recorded in relation with the corona point current obtained during the testing.

It should be noted that, concurrently with the test program herein reported, a series of natural charging current measurements were performed by the U. S. Army TRECOM using the same aircraft under cognizance of Lt. James Seibert, U. S. Army TRECOM. Natural charging currents up to 22 micro-amperes were recorded when flying at extremely low altitudes (below 10 feet). This increase of the natural charging current is attributed to the increase of sand and dust recirculation that exist for such low altitude hovering flight conditions.

f. The dynamic neutralizer discharging system may be used to determine the presence of voltage in the heli-copter by reading the difference of the currents flowing through the positive and negative corona points. If these two corona points are the only ones operating in the aircraft, then its differential current equals the natural charging current when the aircraft potential remains at a steady value.

III. BIBLIOGRAPHY

1. Cierva, Juan de la, Helicopter Static Electricity Discharging Device, Final Report, Project 9R38-01-017-30, Contract DA 44-177-TC-728, TCREC Report 62-33, to be published.

2. Fradenburgh, Evan A., Flow Field Measurements for a Hovering Rotor Near the Ground, American Helicopter Society Fifth Annual Western Forum, Los Angeles, California, September 1958.

3. Poteate, S. Blair, Jr., Accumulation and Dissipation of Static Electricity in Helicopters, Journal of the American Helicopter Society, Vol. 7 No. 2, April 1962.

4. Tona, C. J., Automatic Control of Static Electricity for Army Helicopters, Phase I Report, Project 9R38-01-017-30, Contract DA 44-177-TC-652, TCREC Technical Report 61-18, February 1961.

APPENDIX I

CORONA POINT PROBE DESIGN

KELLETT DRAWINGS

227-73001

227-73102

227-73103

227-73104

BLANK PAGE

Bobin

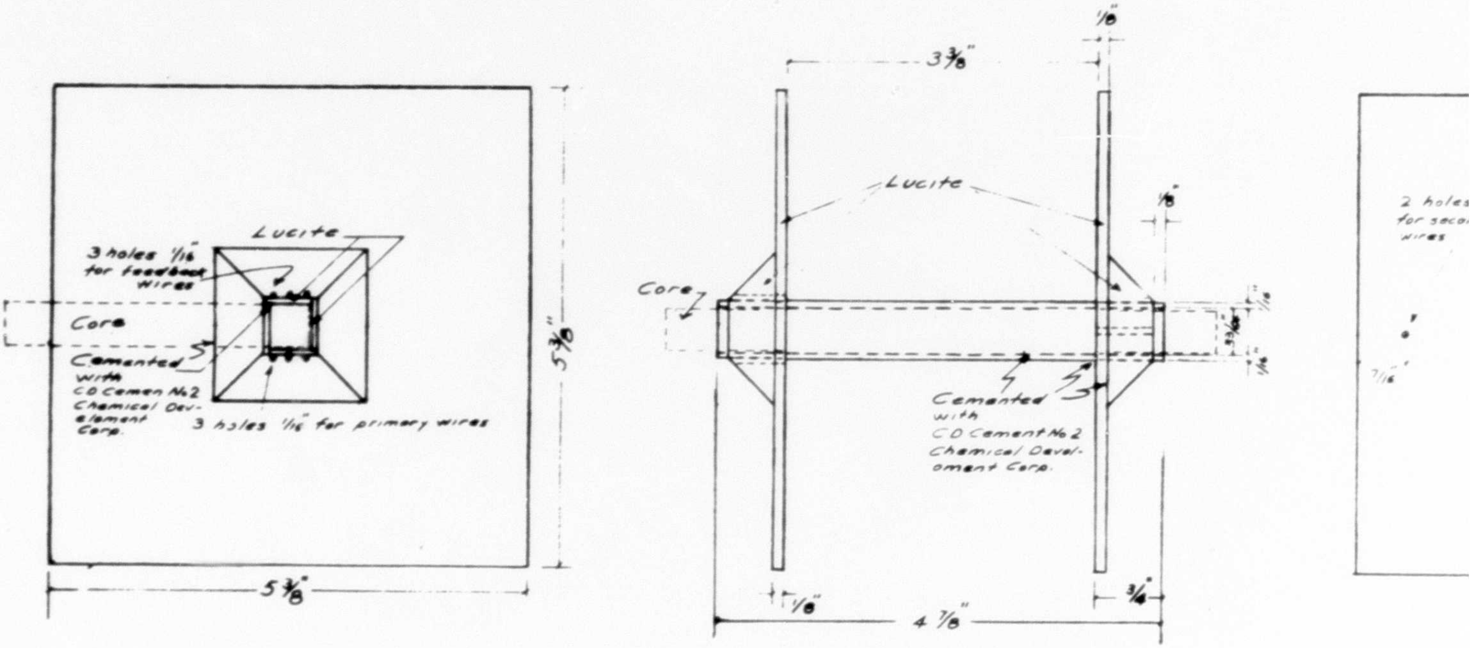

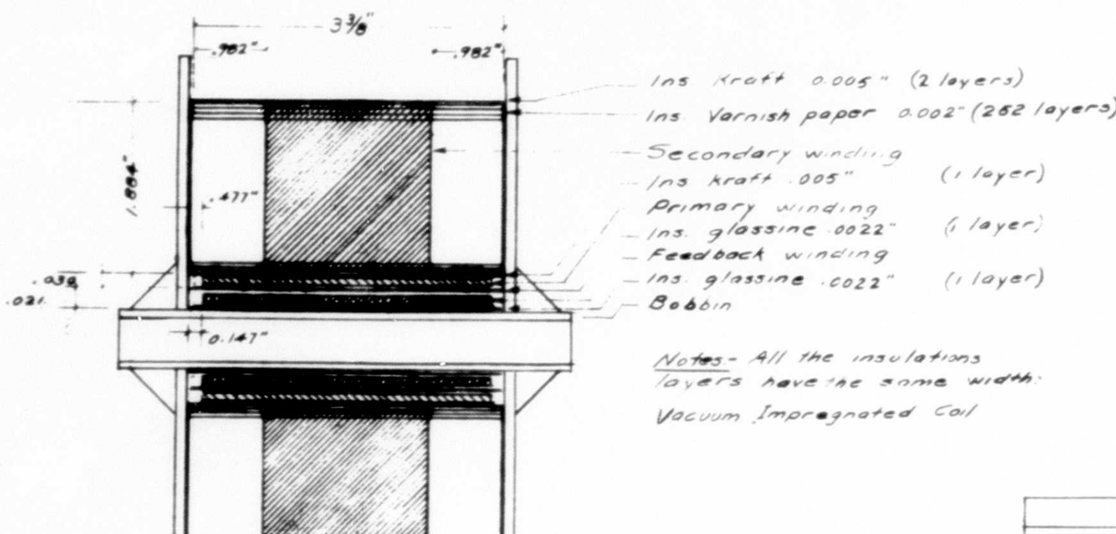

Notes- All the insulations layers have the same width.
Vacuum Impregnated Coil

Winding
(without scale)

	Fe
Wire	# 2
Total Turns	
Layers	
Turns/Layer	
Insulation	0.002
Taps	1 Ce
Margin	0.

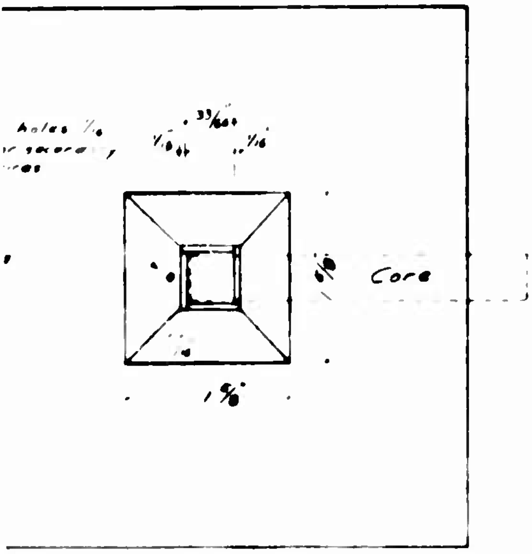

Core

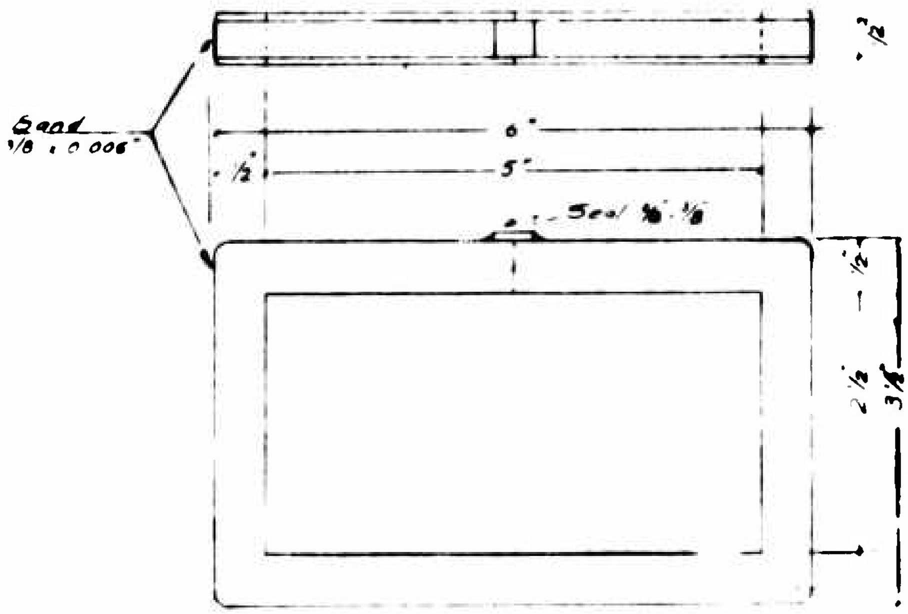

2 mils strips impregnated

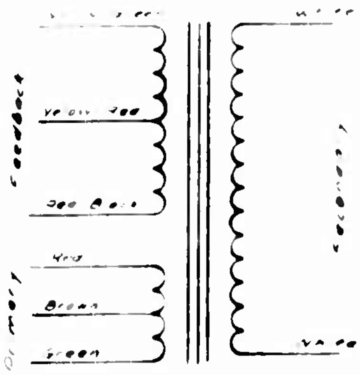

Electric Diagram

Feedback	Primary	Secondary
# 26 SE	# 22 SE	# 36 SE
160	80	55000
		252
160	80	218
0.0022" glass	.005" kraft	0.002" varnish
1 Center tap	1 Center tap	none
0.147	0.477"	0.982"

CORP.

PENNA

Static Electricity Discharger
High Voltage Transformer

Dwg. 227

Bobin

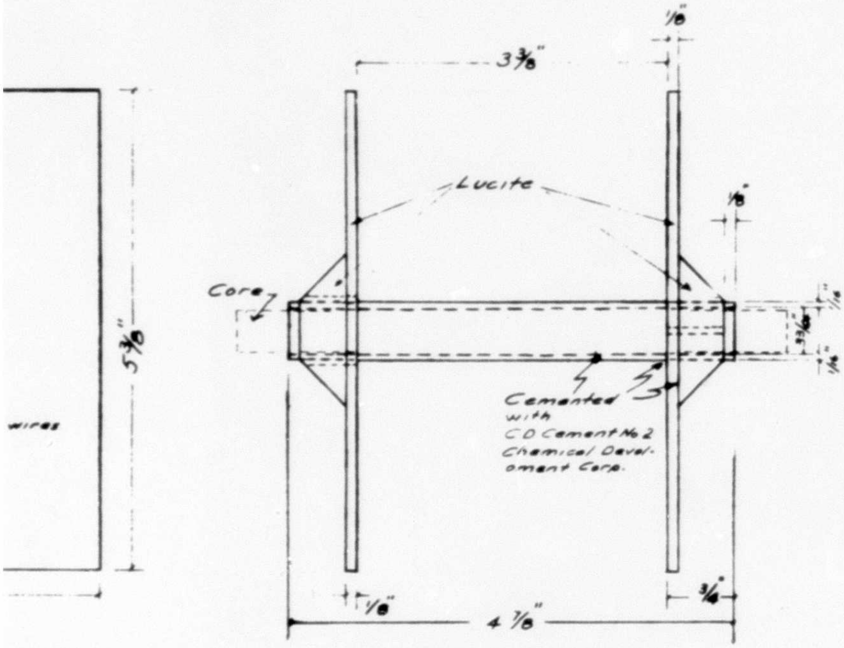

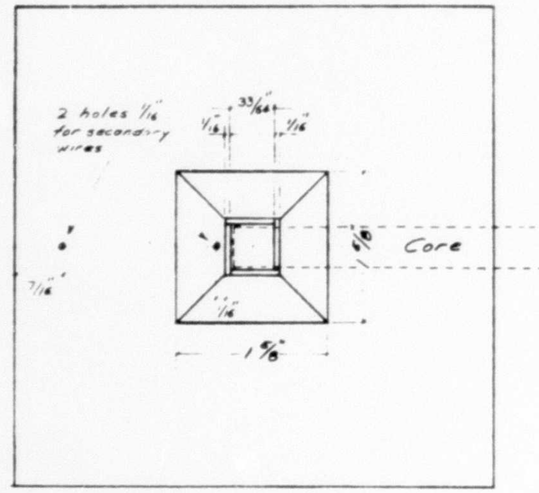

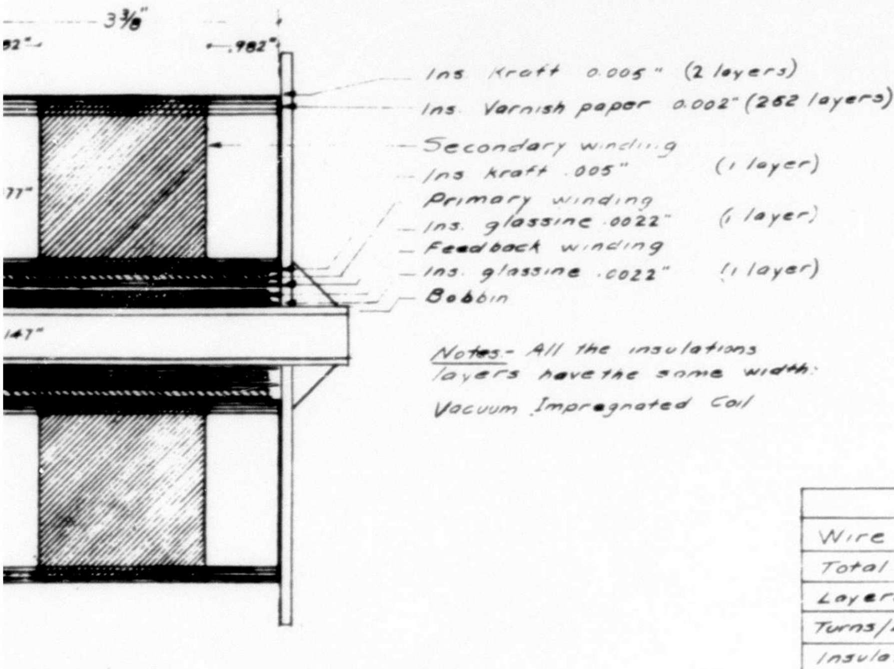

Winding
(without scale)

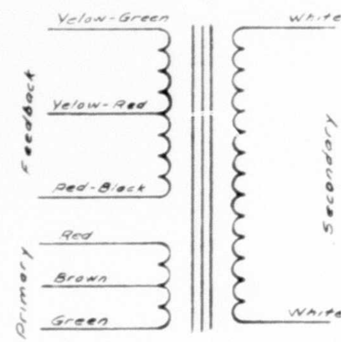

Electric Diagram

Winding Data

	Feedback	Primary	Seconda
Wire	# 26 SE	# 22 SE	# 36 SE
Total Turns	160	80	55000
Layers	1	1	252
Turns/Layer	160	80	218
Insulation	0.0022" glassine	0.005" Kraft	0.002" Varnis
Taps	1 Center tap	1 Center Tap	none
Margin	0.147"	0.477"	0.982"

B

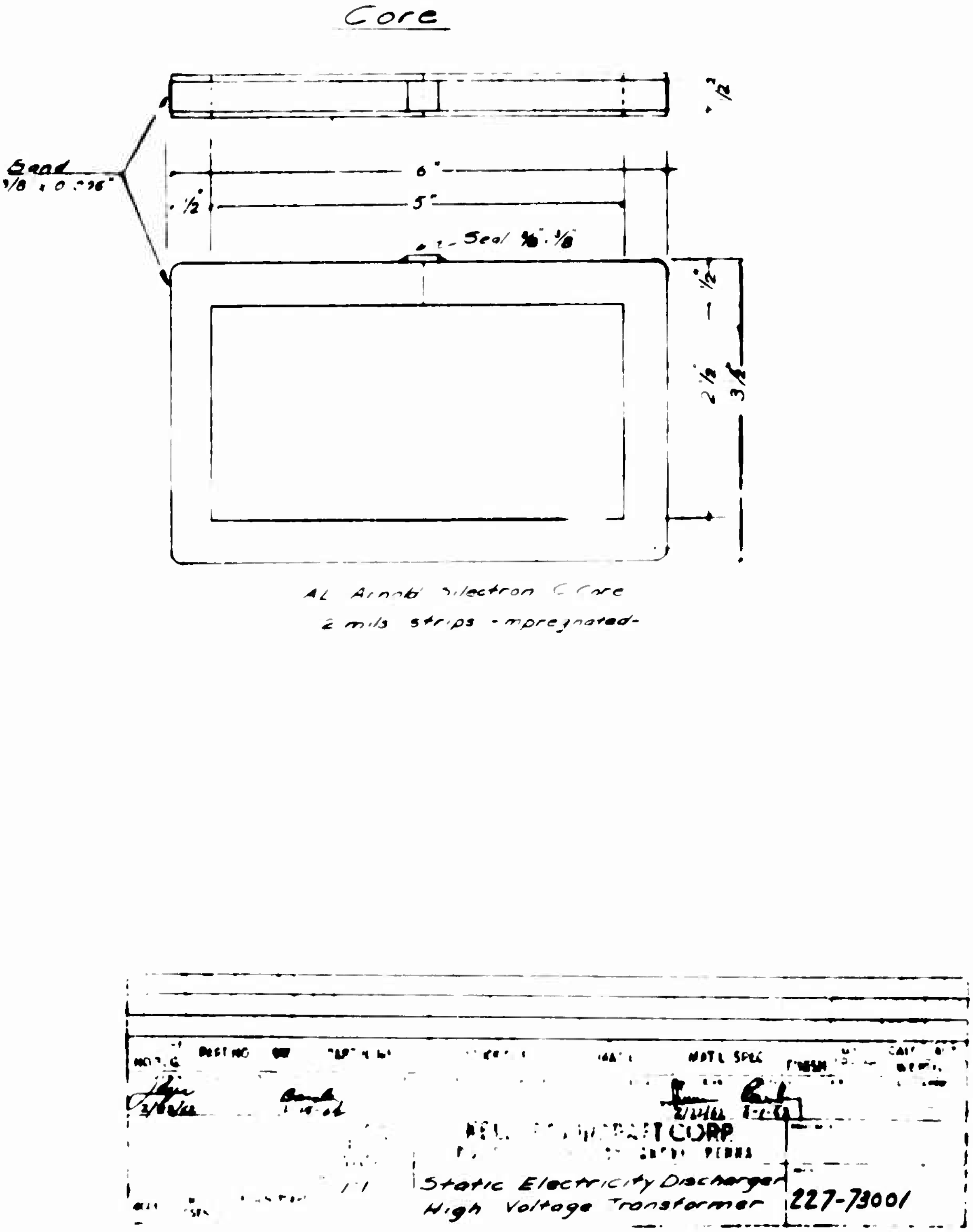

Dwg. 227-73001

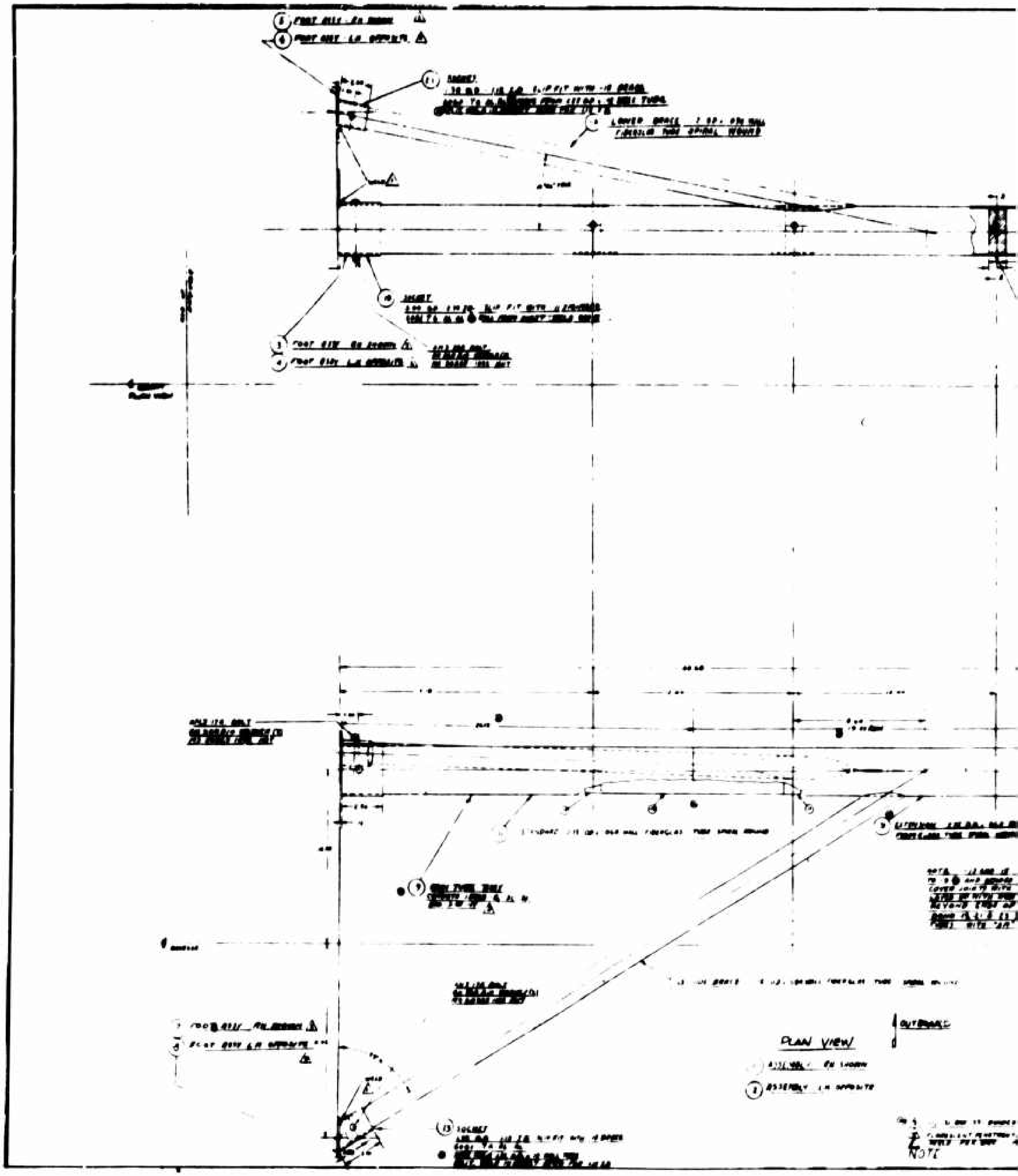

A

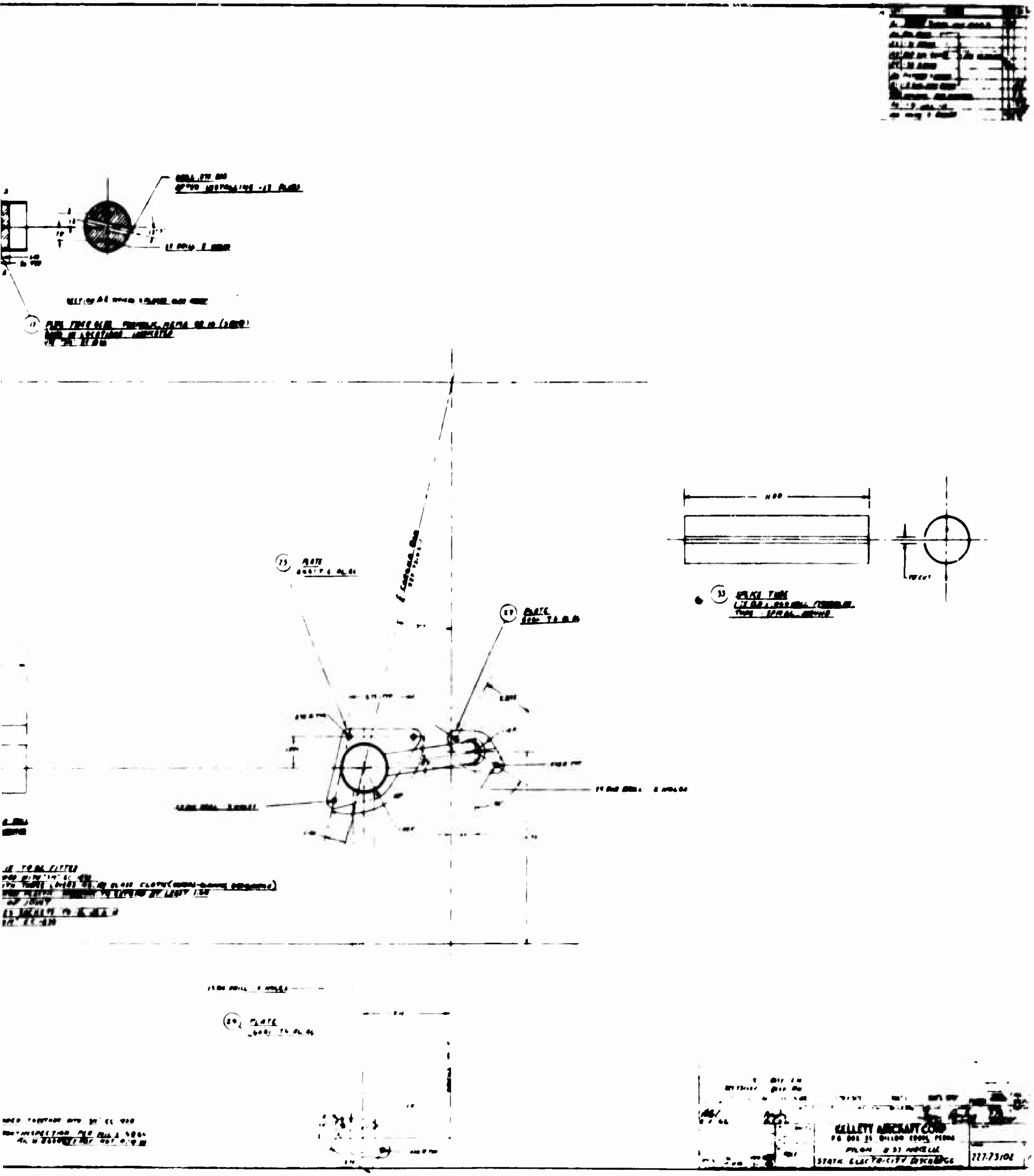

Dwg. 227-73102

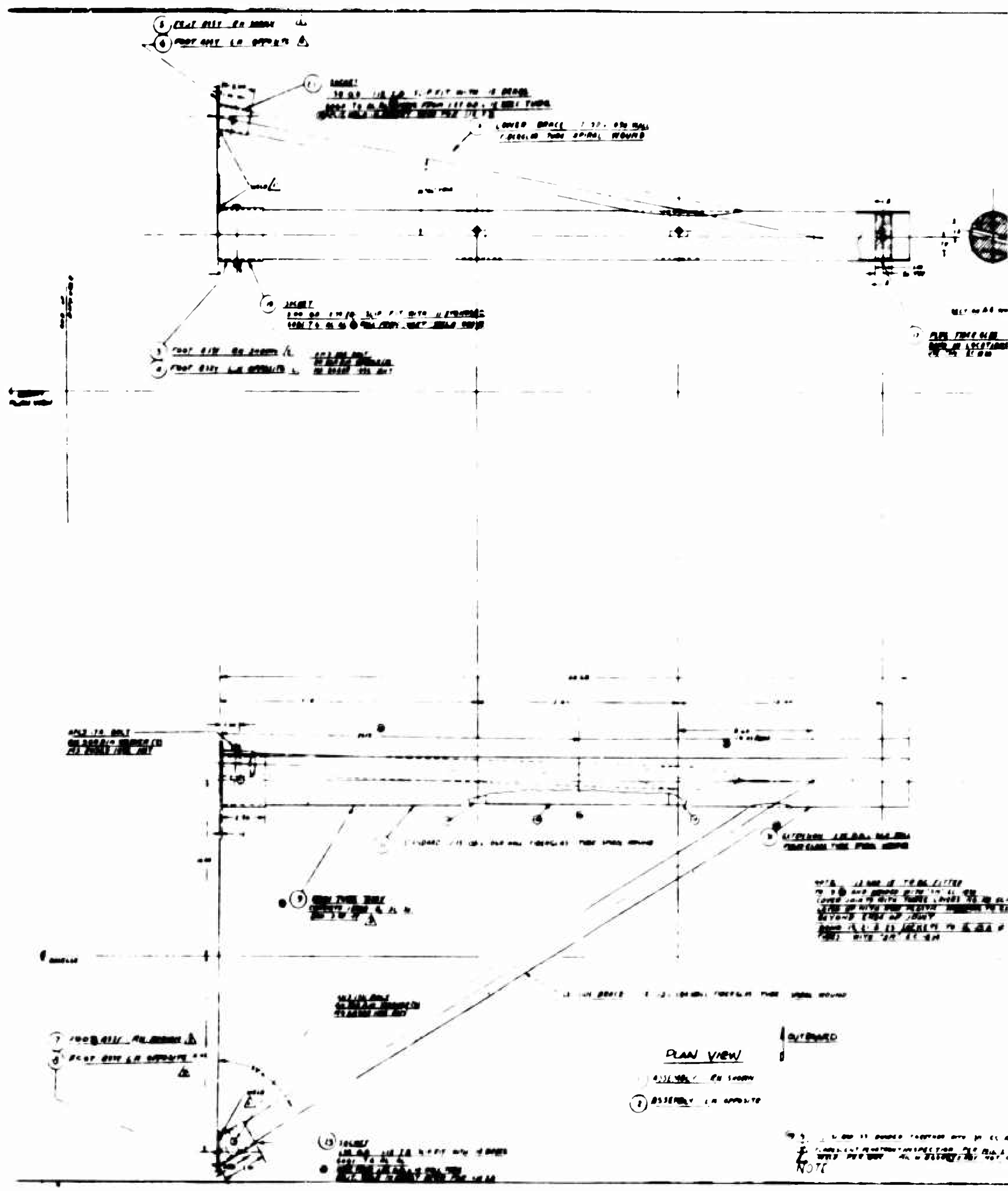

B

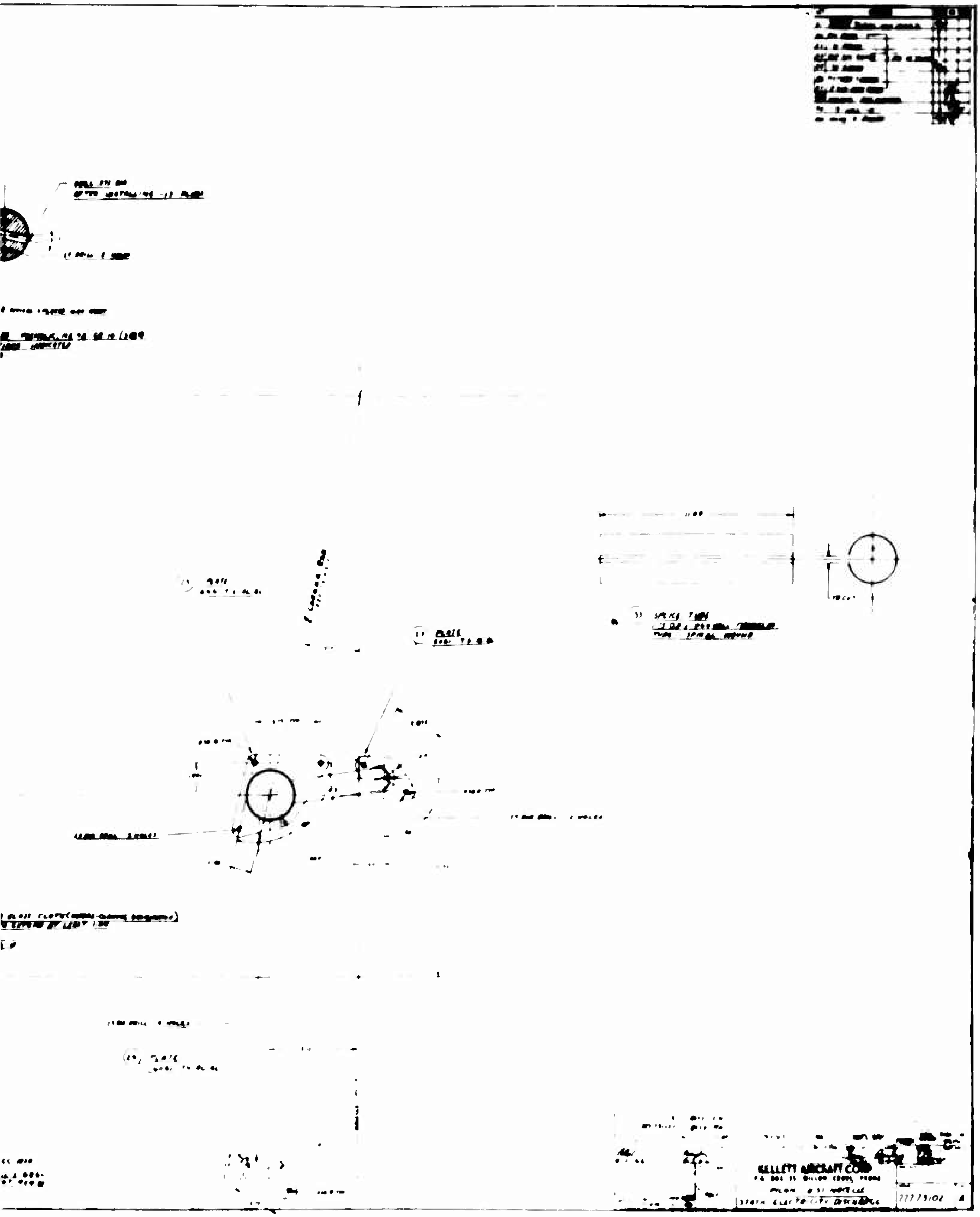

Dwg. 227-73102

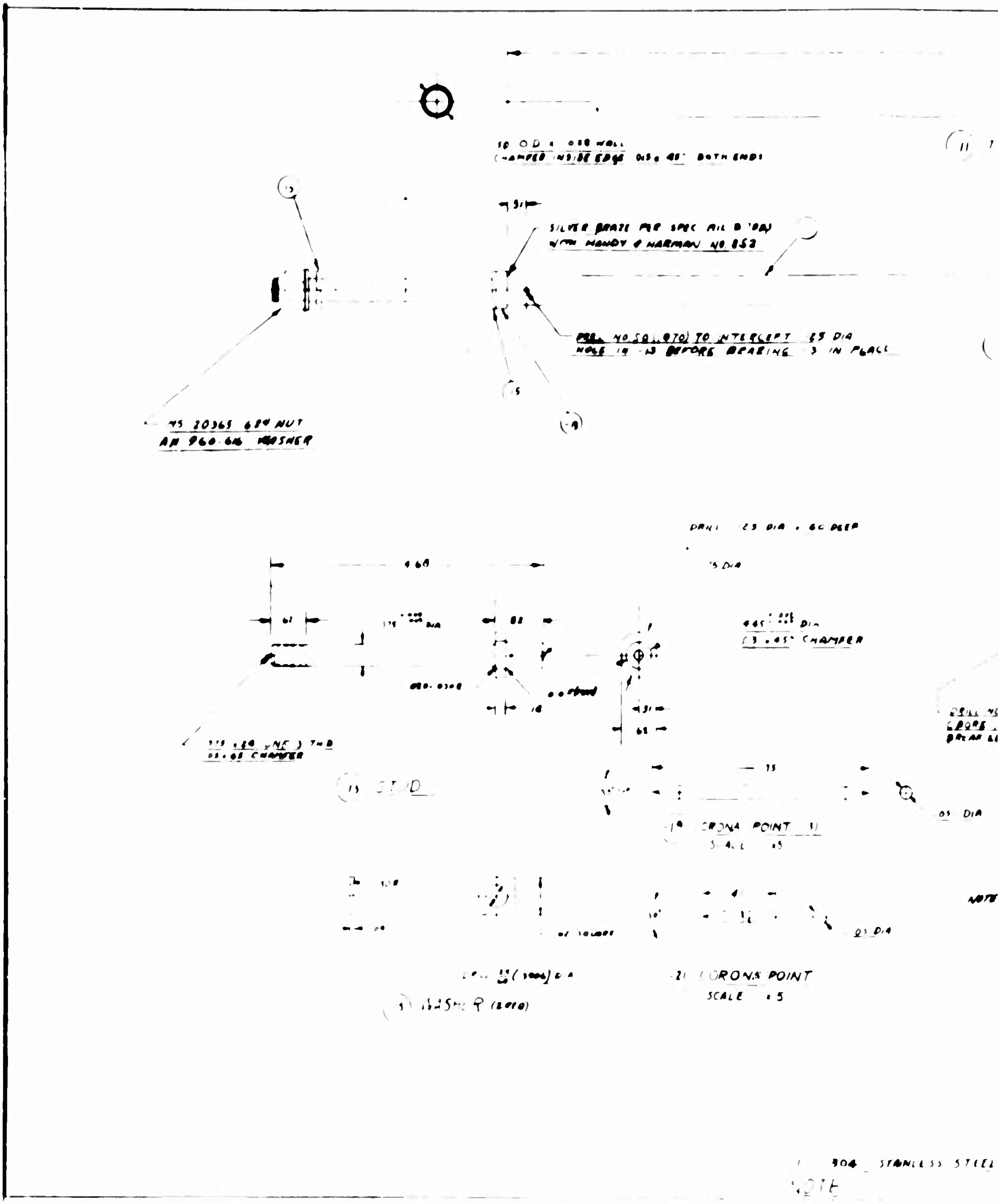

CHAMFER INSIDE EDGE
BOTH ENDS
SILVER BRAZE PER SPEC
WITH HANDY & HARMAN
TO INTERCEPT
BEFORE BEARING
IN PLACE
AN 960 WASHER
DIA x .60 DEEP
CHAMFER
STUD
CORONA POINT
SCALE
CORONA POINT
SCALE
304
STAINLESS STEEL
NOTE

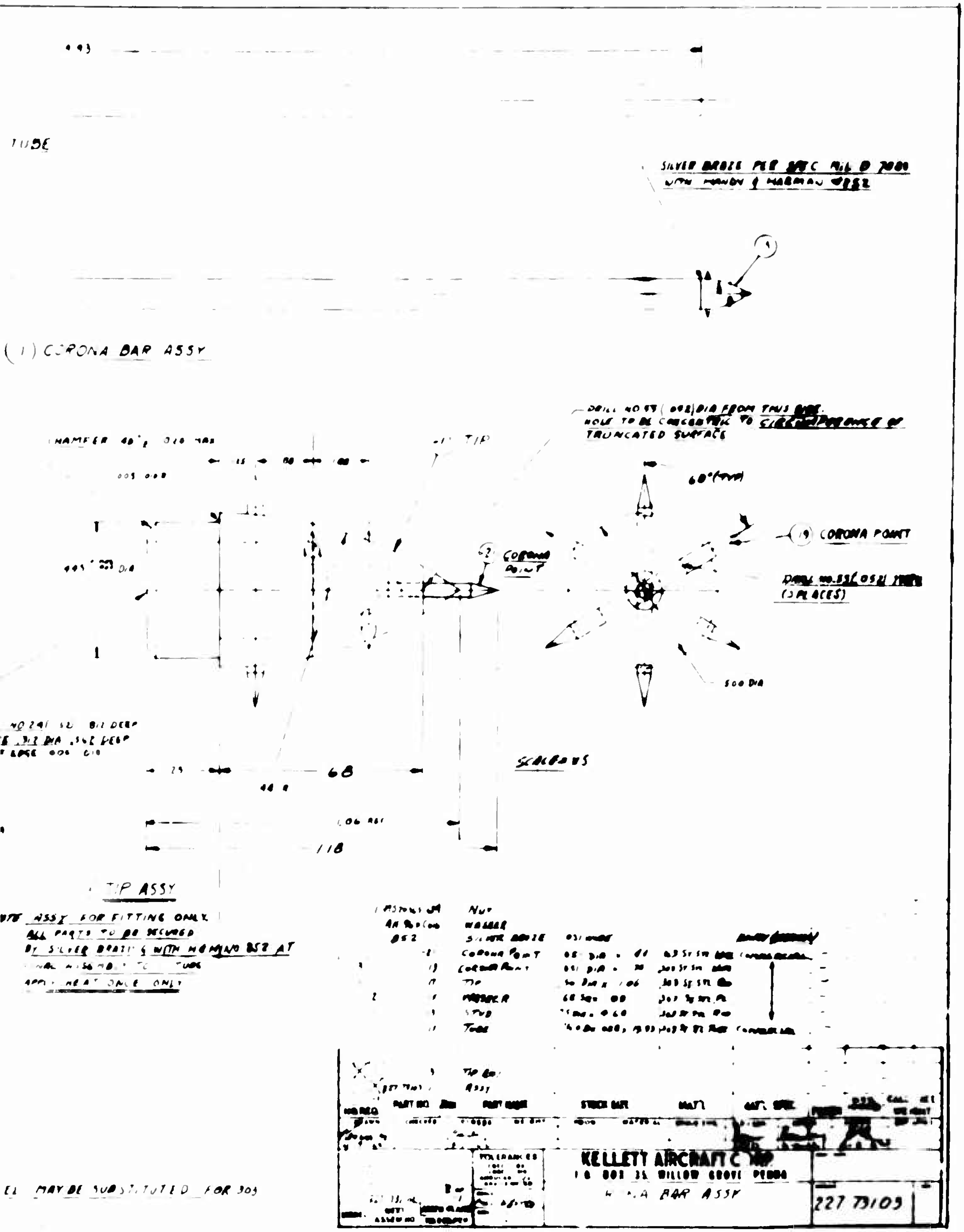

Dwg. 227-73103

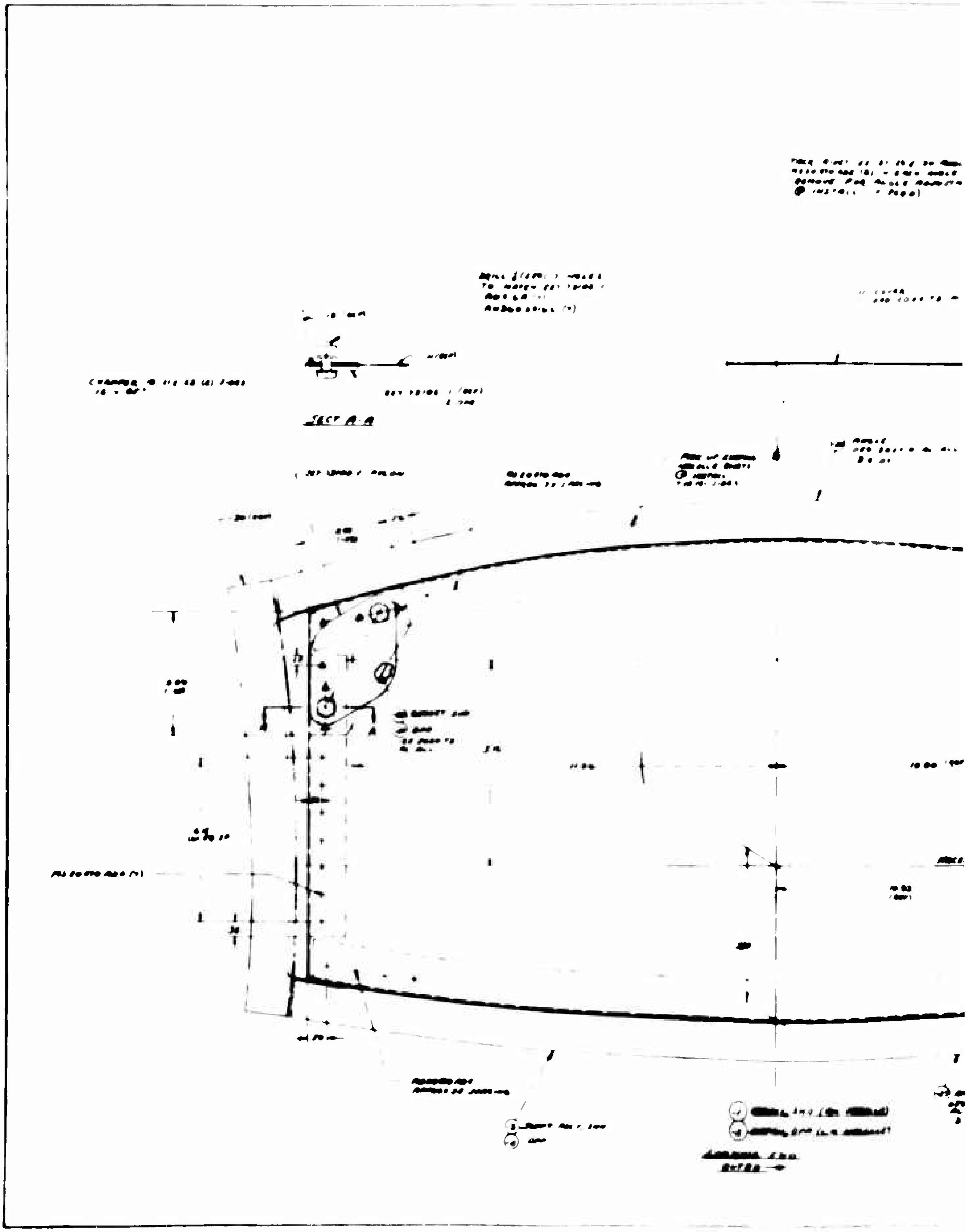
SECT A-A

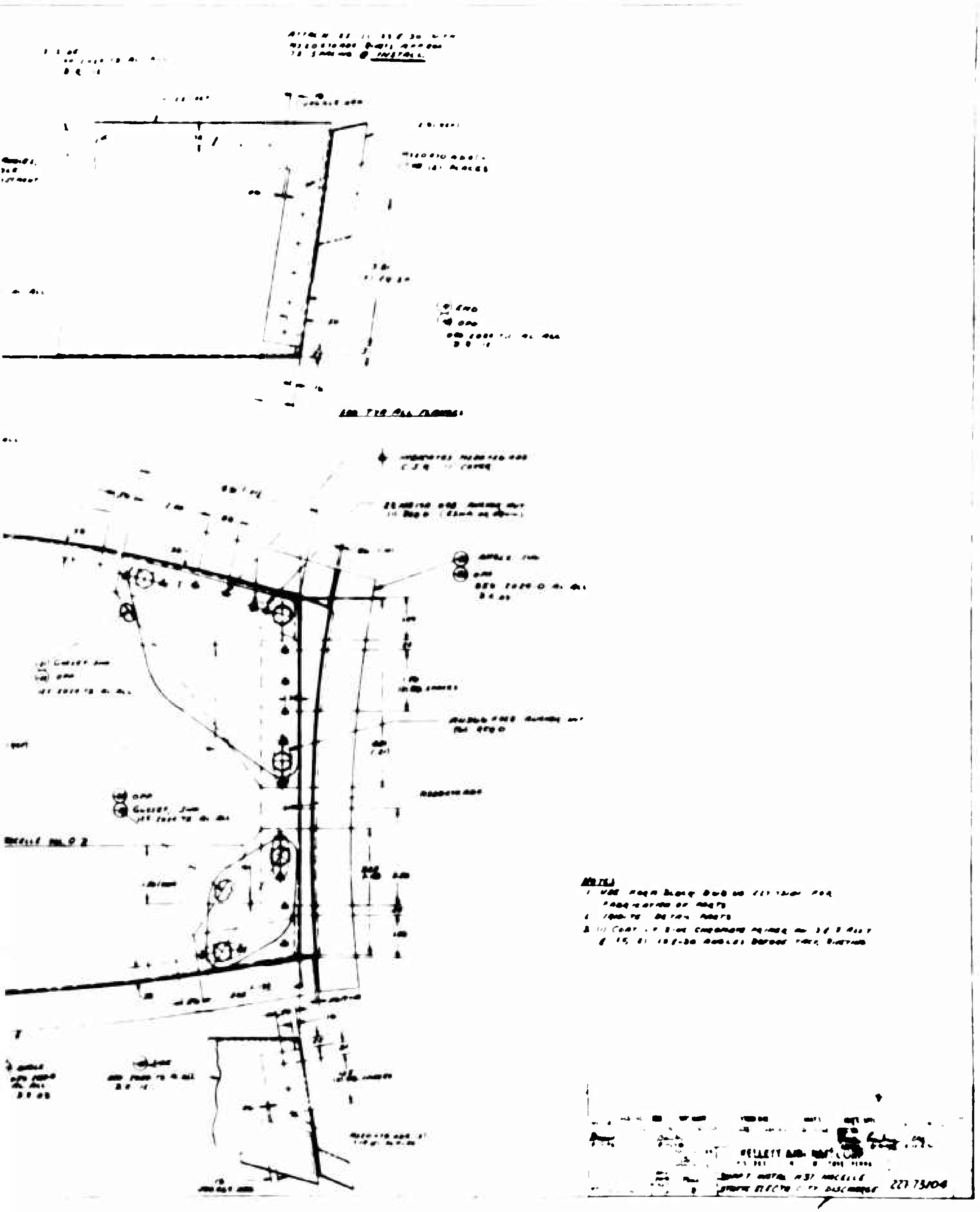

Dwg. 227-73104

BLANK PAGE

DISTRIBUTION

USCONARC	3
Seventh US Army	1
USAIC	2
USACGSC	1
USAWC	1
USAATBD	1
USAAVNBD	1
USATMC(FTZAT), ATO	1
ARO, Durham	2
OCRD, DA	1
NATC	2
ARO, OCRD	1
TO, USAAVNC	1
USAAVNS, CDO	1
CECDA	1
USATCDA	1
USATB	1
USATMC	21
USATFA	1
USATC&FF	4
USATSCH	3
USATRECOM	17
USA Tri-Ser Proj Off	1
TCLO, USAABELCTBD	1
USATRECOM LO, USARDG (EUR)	1
TCLO, USAAVNS	1
USARPAC	1
AFSC (SCS-3)	1
Air Univ Lib	1
AFSC (Aero Sys Div)	2
ASD (ASRMPT)	1
ONR	3
BUWEPS, DN	5
ACRD(OW), DN	1
USNPGSCH	1
CMC	1
MCLFDC	1
MCEC	1
MCLO, USATSCH	1
NAFEC	3

Langley Rsch Cen, NASA	2
Ames Rsch Cen, NASA	2
Lewis Rsch Cen, NASA	1
Sci & Tech Info Fac	1
ASTIA	10
USASRDL	2
USAMOCOM	3
Kellett Acft Corp.	10
USAMC	4
USAMCAFO	1
Marine Acft Gp 36	1
SG	1
USSTRICOM	1